Open access • Journal Article • DOI:10.1103/PHYSREVA.47.642

Quantum theory of field-quadrature measurements. — Source link

Howard M. Wiseman, Gerard J. Milburn

Institutions: University of Queensland

Published on: 01 Jan 1993 - Physical Review A (American Physical Society)

Topics: Homodyne detection, Quantum nondemolition measurement, Squeezed coherent state, Quantum optics and State vector

Quantum theory of field-quadrature measurements

H. M. Wiseman and G. J. Milburn
Department of Physics, University of Queensland, Queensland 4072, Australia
(Received 5 June 1992; revised manscript received 21 July 1992)

The quantum effects on a cavity mode of the electromagnetic field caused by measuring one of its quadrature components is analyzed. We consider three measurement schemes: an intracavity quantum-nondemolition coupling to another mode, simple homodyne detection, and balanced homodyne detection. It is shown that, for suitable initial conditions, the first scheme has an effect which approaches that of a projective collapse of the state vector for long measurement times. However, the two homodyne schemes (which are shown to be equivalent for large local-oscillator amplitudes) do not approximate a projective measurement in any limit. In particular, it is shown that homodyne measurement cannot produce a squeezed state from a classical initial state. All three schemes are analyzed in terms of "quantum trajectories" which link measurement theory with stochastic quantum-jump processes.

PACS number(s): 42.50.Lc, 03.65.Bz, 42.50.Dv, 42.50.Ar

I. INTRODUCTION

It has been recognized for some time [1] that standard photon-counting measurements in quantum optics are not describable in terms of the projection postulate of traditional quantum-measurement theory [2]. However, one still finds standard (homodyne) field-quadrature measurements treated in this way [3, 4]. This approach is analogous with ideal position or momentum measurements on a particle in a harmonic potential well. Such formal, projective measurements actually leave the system in a state of infinite energy. This is clearly in contradiction with external homodyne measurements of a cavity field, because no energy is injected into the cavity, and in fact energy must be lost in order for a signal to be detected.

In this paper, we investigate three schemes for measuring the X_1 quadrature of a cavity field. The first, presented in Sec. III, is a quantum-nondemolition (QND) measurement of X_1 via a coupling to the field of another, heavily damped mode. It is shown that, for suitable initial conditions, this measurement does approximate a projective one, with the state of the cavity asymptotically approaching an X_1 eigenstate as the time of measurement goes to infinity.

Simple homodyne measurements (SHM) are analyzed in Sec. IV, and balanced homodyne measurements (BHM) in Sec. V. For large local-oscillator amplitudes, these two schemes give identical results. It is shown that, as expected, the projection postulate does not apply to such measurements. In particular, classical states (having a positive Glauber-Sudarshan P representation [5,6]) remain classical states under homodyne detection. Nevertheless, it is found that, for certain nonclassical initial conditions, a squeezed state (variance of X_1 less than 0.25) is typically produced in the cavity over some range of measurement times. As the measurement time goes to infinity, however, the system relaxes into a vacuum state.

In modeling these three schemes of quadrature measurements, the concept of quantum trajectories, due to Carmichael [7, 8], is used extensively. This theory, introduced in Sec. II, allows nonunitary evolution, which is normally described by a master equation for a density operator, to be treated using stochastic trajectories for a pure state. If the nonunitary evolution describes a measurement process, then this pure state has an interpretation as the actual state of the system conditioned on the results of the measurement. The stochastic trajectories are particularly useful for doing numerical simulations of otherwise intractable problems such as homodyne measurements.

II. PHOTODETECTION HISTORIES AND QUANTUM TRAJECTORIES

Consider a single-mode field in a cavity with linewidth γ due to partial transmission through one mirror, and with internal dynamics governed by a Liouville superoperator $\mathcal{L}_0$. The density operator for that mode obeys the following master equation in the interaction picture:

$$\dot{\rho} = \mathcal{L}_0\rho + \frac{\gamma}{2}(2a\rho a^\dagger - a^\dagger a\rho - \rho a^\dagger a) \equiv \mathcal{L}\rho. \tag{2.1}$$

The formal solution to this equation is

$$\rho(t) = e^{\mathcal{L}t}\rho(0). \tag{2.2}$$

The superoperator $\mathcal{L}$ can be split into two terms: $\mathcal{L} = \mathcal{J} + (\mathcal{L} - \mathcal{J})$, where the action of $\mathcal{J}$ is defined by

$$\mathcal{J}\rho \equiv C\rho C^\dagger, \tag{2.3}$$

where C is the output field from the cavity, ignoring vacuum fluctuations [9],

$$C = \sqrt{\gamma}\,a. \tag{2.4}$$

Evidently, the instantaneous rate of photon counting at a detector of unit efficiency placed at the output of the cavity is equal to $\langle C^\dagger C\rangle = \mathrm{Tr}[\mathcal{J}\rho(t)]$.

Now, we can use a generalized Dyson expansion for superoperators [10] to write Eq. (2.2) as follows:

$$\rho(t) = \sum_{m=0}^{\infty} \int_0^t dt_m \int_0^{t_m} dt_{m-1} \cdots \int_0^{t_2} dt_1 \mathcal{S}(t-t_m)\mathcal{J}\mathcal{S}(t_m - t_{m-1}) \cdots \mathcal{J}\mathcal{S}(t_1)\rho(0), \tag{2.5}$$

where we have defined $\mathcal{S}(t) = e^{(\mathcal{L}-\mathcal{J})t}$ in line with the notation of Srinivas and Davies [1]. In this expansion, the choice of superoperator $\mathcal{J}$ is obviously arbitrary. However, for the definition of $\mathcal{J}$ given above (2.3) in terms of output fields from the cavity incident on a perfect photodetector, the terms in (2.5) have a unique physical significance. It is shown in Ref. [10] that the probability for such a detector, operational in the time interval $[0,t]$, to record exactly m detections, one in each of the disjoint, infinitesimal time intervals times $[t_1, t_1 + dt_1], ..., [t_m, t_m + dt_m] \in [0,t]$ is given by

$$p_m(t_1, ..., t_m; [0,t])dt_1, ..., dt_m = \mathrm{Tr}[\mathcal{S}(t-t_m)\mathcal{J}\mathcal{S}(t_m - t_{m-1}) \cdots \mathcal{J}\mathcal{S}(t_1)\rho(0)]dt_1, ..., dt_m, \tag{2.6}$$

where $\rho(0)$ gives the initial state of the cavity mode (the time delay due to the finite propagation time outside the cavity is ignored). If we define a non-normalized, conditional density operator $\tilde{\rho}_c(t)$, conditioned on the photocount record defined above, by

$$\tilde{\rho}_c(t) = \mathcal{S}(t-t_m)\mathcal{J}\mathcal{S}(t_m - t_{m-1}) \cdots \mathcal{J}\mathcal{S}(t_1)\rho(0), \tag{2.7}$$

then we see that the exclusive probability density is simply given by

$$p_m(t_1, ..., t_m; [0,t]) = \mathrm{Tr}[\tilde{\rho}_c(t)]. \tag{2.8}$$

Denoting the normalized conditional density operator by $\rho_c(t)$, the unconditional density operator at time t is then given by, from (2.5),

$$\rho(t) = \sum_{m=0}^{\infty} \int_0^t dt_m \int_0^{t_m} dt_{m-1} \cdots \int_0^{t_2} dt_1 p_m(t_1, ..., t_m; [0,t])\rho_c^{(m;t_1,...,t_m)}(t). \tag{2.9}$$

Thus, the conditional density operator $\rho_c(t)$ can be interpreted as representing the actual state of the system, given the photodetection history. The unconditional density operator is an ensemble average of these conditional states, weighted by the probabilities of recording the particular sequence of photodetections.

Often the simplest way to generate these sequences, and there corresponding conditional system states, with the correct probabilities, is to do numerical simulations. The method outlined below is due to Carmichael, who terms each simulation a "quantum trajectory." As yet, there is no formal proof of the equivalence of an ensemble of quantum trajectories to that in (2.9), but there is a wealth of supporting numerical evidence [7, 8].

It is easily shown [7] that the probability to detect a photon in the time interval $[t, t+dt]$, given the previous detection history, is

$$p_c dt = \mathrm{Tr}[\mathcal{J}\rho_c(t)]dt, \tag{2.10}$$

as expected. Using a numerical simulation with a finite-time step Δt, one thus generates a random number r on the unit interval, evolves the state forward according to

$$\tilde{\rho}_c(t+\Delta t) = \mathcal{J}\rho_c(t)\Delta t \quad \text{if} \quad r \le p_c \Delta t, \tag{2.11}$$

in which case a photodetection is recorded to have occurred in the interval $[t, t+\Delta t]$, or

$$\tilde{\rho}_c(t+\Delta t) = \mathcal{S}(\Delta t)\rho_c(t) \quad \text{if} \quad r > p_c \Delta t, \tag{2.12}$$

when no photon is detected. The tilde in these equations indicates that the density operator thus produced is unnormalized, and must be normalized before the next calculation of (2.10).

If, as is often the case, the output coupling of the cavity mode is the only nonunitary dynamics of the system, then the numerical simulation can be further simplified, and its interpretation as a quantum trajectory tightened. When $\mathcal{L}_0$ in Eq. (2.1) is defined by $i\hbar\mathcal{L}_0\rho \equiv [H_0, \rho]$, the superoperator $\mathcal{S}(t)$ can be written as

$$\mathcal{S}(t)\rho = N(t)\rho N^\dagger(t), \tag{2.13}$$

where $N(t)$ is a nonunitary operator given by

$$N(t) = \exp\left[\left(\frac{1}{i\hbar}H_0 - \tfrac{1}{2}\gamma a^\dagger a\right)t\right]. \tag{2.14}$$

In this case, both $\mathcal{J}$ and $\mathcal{S}(t)$ preserve pure states. That is, they transform a ray in Hilbert space into another ray. Thus, if the system is initially pure, then the entire quantum trajectory can be done in terms of conditioned state vectors $|\psi_c(t)\rangle$ rather than density operators. Equations (2.10)–(2.12) are simply replaced by

$$p_c = \langle\psi_c(t)|C^\dagger C|\psi_c(t)\rangle, \tag{2.15}$$

$$|\tilde{\psi}_c(t+\Delta t)\rangle = C|\psi_c(t)\rangle\sqrt{\Delta t} \quad \text{if} \quad r \le p_c\Delta t, \tag{2.16}$$

$$|\tilde{\psi}_c(t+\Delta t)\rangle = N(\Delta t)|\psi_c(t)\rangle \quad \text{if} \quad r > p_c\Delta t. \tag{2.17}$$

This model makes it clear that the density-operator formalism is only required when our knowledge of the system dynamics is incomplete. When the irreversible loss of a photon is detected at a precise time, then we have full knowledge of the change of state of the system,

and it remains pure. In addition to the conceptual appeal of quantum trajectories as pure states, there is the computational advantage that a ket vector in N-dimensional Hilbert space requires only $2N-1$ real numbers to define, compared to N^2-1 for a density matrix.

If the measurement provides incomplete knowledge of the irreversible processes in the system, then $\mathcal{S}(t)$ will no longer preserve pure states. For example, if the photodetector has efficiency η then $\mathcal{J}$ is defined by $\mathcal{J}\rho = \eta C\rho C^\dagger$, and $\mathcal{S}(t) = e^{(\mathcal{L}-\mathcal{J})t}$ can no longer be factorized as in (2.13). In this case, the density matrix and equations (2.10)–(2.12) must be used in the quantum trajectory. Alternatively, $\mathcal{J}$ may be retained as before, but each "jump" has only a probability η of being recorded as a photodetection. In this case, the state vector is now conditioned on unknown events, and the notion of a quantum trajectory loses some of its meaning. We will use the terms "strict quantum trajectory" to denote a simulation in which each jump has an exact correspondence with a recorded event (e.g., a photodetection), and "lax quantum trajectory" in other cases.

III. QUANTUM-NONDEMOLITION QUADRATURE MEASUREMENT

In this section we present a model for achieving a quantum-nondemolition measurement of the X_1 quadrature of a cavity field. By this we mean that the statistics for the measured quantity (X_1) are not changed by the measurement in the nonselective (unconditional) case. It is shown that, for suitable initial conditions, the field is left in an eigenstate of X_1 after the measurement. Analytical and numerical results are presented.

A. Master equation for QND quadrature measurement

The model for measuring the X_1 quadrature for a cavity mode, first proposed in Ref. [11], is shown in Fig. 1. The cavity supports two modes of different frequencies, with annihilation operators a and b. The a mode is the system, while the heavily damped b mode is part of the measuring apparatus. The two modes are coupled by the following nonlinear Hamiltonian (in the interaction picture):

$$H = \hbar\chi X_1 Y_1, \tag{3.1}$$

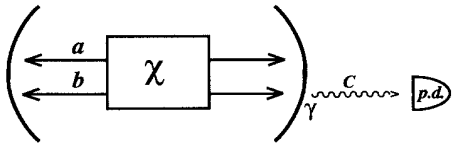

FIG. 1. Diagram of the QND-measurement scheme for the X_1 quadrature. The $\chi^{(2)}$ nonlinearity of the crystal couples the X_1 quadrature of the a mode (the system) to that of the b mode. The b mode is heavily damped at a rate γ and together with the photodetector (p.d.) forms the apparatus.

where $X_1 = (a + a^\dagger)/2$ and $Y_1 = (b + b^\dagger)/2$, and χ is assumed real for simplicity. This could be achieved by, for example, a crystal with a $\chi^{(2)}$ nonlinearity in which two processes driven by classical fields, amplification ($\varepsilon_s^* ab$+H.c., with $\omega_s = \omega_a + \omega_b$), and frequency conversion ($\varepsilon_d^* ab^\dagger$+ H.c., with $\omega_d = \omega_a - \omega_b$) have equal strengths. Mode b is damped through an output mirror at rate γ, and the output enters a perfect photodetector. Mode a may have some internal dynamics defined by its Liouville superoperator $\mathcal{L}_0$. The density operator for both modes obeys the following master equation:

$$\dot{W} = \mathcal{L}_0 W - i\chi[X_1 Y_1, W] + \frac{\gamma}{2}(2bWb^\dagger - b^\dagger bW - Wb^\dagger b) \equiv \mathcal{L}W. \tag{3.2}$$

We now assume that mode b is so heavily damped that (apart from initial transients) it has few photons and will be slaved to mode a. This will allow the dynamics of mode b to be eliminated adiabatically as in Ref. [12], resulting in a master equation for mode a alone. Specifically, we assume that

$$\left|\frac{\langle\mathcal{L}_0\rangle}{\gamma}\right| \sim \left|\frac{\chi\langle X_1\rangle}{\gamma}\right| = \epsilon \ll 1. \tag{3.3}$$

Now, we can expand W in powers of ϵ:

$$W = \rho_0 \otimes |0\rangle_b\langle 0| + (\rho_1 \otimes |1\rangle_b\langle 0| + \text{H.c.}) + \rho_2 \otimes |1\rangle_b\langle 1| + (\rho_{2'} \otimes |2\rangle_b\langle 0| + \text{H.c.}) + O(\epsilon^3) \tag{3.4}$$

Here the subscripts on the density operators $\rho_0, \rho_1, \rho_2, \rho_{2'}$ for mode a indicate orders of magnitude in ϵ. This expansion will be shown to be consistent with the assumption (3.3). Substituting (3.4) into the master equation (3.2) gives

$$\dot{\rho}_0 = \mathcal{L}_0\rho_0 - \frac{i\chi}{2}[X_1\rho_1 - \rho_1^\dagger X_1] + \gamma\rho_2, \tag{3.5}$$

$$\dot{\rho}_1 = \mathcal{L}_0\rho_1 - \frac{i\chi}{2}[X_1\rho_0 + \sqrt{2}X_1\rho_{2'} - \rho_2 X_1] - \frac{\gamma}{2}\rho_1 + \gamma O(\epsilon^4), \tag{3.6}$$

$$\dot{\rho}_2 = \mathcal{L}_0\rho_2 - \frac{i\chi}{2}[X_1\rho_1^\dagger - \rho_1 X_1] - \gamma\rho_2 + \gamma O(\epsilon^4), \tag{3.7}$$

$$\dot{\rho}_{2'} = \mathcal{L}_0\rho_{2'} - \frac{i\chi}{2}[\sqrt{2}X_1\rho_1] - \gamma\rho_{2'} + \gamma O(\epsilon^4). \tag{3.8}$$

By examination of (3.6) and (3.8) we see that the off-diagonal elements ρ_1 and $\rho_{2'}$ can be adiabatically eliminated by slaving them to the on-diagonal elements ρ_0 and ρ_2. Putting $\dot{\rho}_{2'} = 0$ under assumption (3.3) gives

$$\rho_{2'} = \frac{-i\chi}{\sqrt{2}\gamma}X_1\rho_1 + O(\epsilon^3) = O(\epsilon^2). \tag{3.9}$$

Substituting this into (3.6) and putting $\dot{\rho}_1 = 0$ gives

$$\rho_1 = \frac{-i\chi}{\gamma}[X_1\rho_0 - \rho_2 X_1] + O(\epsilon^4) = O(\epsilon). \tag{3.10}$$

Substituting this into (3.5) and (3.7) gives

$$\dot{\rho}_0 = \mathcal{L}_0\rho_0 - \frac{\chi^2}{2\gamma}[X_1^2\rho_0 - X_1\rho_2X_1 + \rho_0X_1^2 - X_1\rho_2X_1] + \gamma\rho_2, \tag{3.11}$$

$$\dot{\rho}_2 = \mathcal{L}_0\rho_0 + \frac{\chi^2}{2\gamma}[X_1\rho_0X_1 - X_1^2\rho_2 + X_1\rho_0X_1 - \rho_2X_1^2] - \gamma\rho_2. \tag{3.12}$$

Now, the reduced density operator for mode a is $\rho = \mathrm{Tr}_b(W) = \rho_0+\rho_2+O(\epsilon^4)$. Thus, adding (3.11) and (3.12) yields the following master equation for the system:

$$\dot{\rho} = \mathcal{L}_0\rho - \frac{\chi^2}{2\gamma}[X_1,[X_1,\rho]] \equiv \mathcal{L}_a\rho. \tag{3.13}$$

The double commutator in this master equation is typical of QND measurements in the continuous limit. It causes the density operator to become diagonal in the basis of the measured quantity (here X_1). This is easily seen from the explicit expression for $\rho(t)$ in the X_1 basis, assuming $\mathcal{L}_0 = 0$:

$$\rho(x,x',t) = \exp\left[-\frac{\Gamma}{2}(x-x')^2t\right]\rho(x,x',0), \tag{3.14}$$

where we have defined $\Gamma = \chi^2/\gamma$.

B. Interpretation as quantum trajectories

If we define a "jump" superoperator for the a mode by

$$\mathcal{J}_a\rho = \Gamma X_1\rho X_1 \tag{3.15}$$

then we can write the formal solution of (3.13) in the form of (2.5),

$$\rho(t) = \sum_{m=0}^{\infty}\int_0^t dt_m\int_0^{t_m}dt_{m-1}\cdots\int_0^{t_2}dt_1\,\mathcal{S}_a(t-t_m)\mathcal{J}_a\mathcal{S}_a(t_m-t_{m-1})\cdots\mathcal{J}_a\mathcal{S}_a(t_1)\rho(0). \tag{3.16}$$

Providing that $\mathcal{L}_0$ is generated by a Hamiltonian H_0, the smooth evolution operator is of the form

$$\mathcal{S}_a(t)\rho = N(t)\rho N(t)^\dagger \tag{3.17}$$

with

$$N(t) = \exp\left[\left(\frac{1}{i\hbar}H_0 - \tfrac{1}{2}\Gamma X_1^2\right)t\right]. \tag{3.18}$$

Then we can consider a particular quantum trajectory in terms of pure states collapsing due to the measurement of X_1 via (3.15) at probabilistically chosen times, and evolving smoothly via (3.17) between jumps.

However, as explained in Sec. II, such a trajectory is only physically meaningful if the history of collapses correspond to some recorded history of events, such as photodetections. The following argument establishes that, under the assumptions of Sec. III A, a jump in the state of mode a via (3.15) does correspond to a detection of a photon in the output field of mode b.

From Eq. (3.12) for $\dot{\rho}_2$, we see that under the adiabatic assumption (3.3), ρ_2 can also be slaved to ρ_0, giving

$$\rho_2 = \frac{\chi^2}{\gamma^2}X_1\rho_0X_1 + O(\epsilon^3) = O(\epsilon^2). \tag{3.19}$$

Thus, to leading order the density operator for mode a is

$$\rho = \rho_0 + \frac{\chi^2}{\gamma^2}X_1\rho_0X_1 \tag{3.20}$$

or

$$\rho_0 = \rho - \frac{\chi^2}{\gamma^2}X_1\rho X_1. \tag{3.21}$$

Substituting this expression into Eqs. (3.9), (3.10), and (3.19) yields the following expression for the density operator (3.4) for modes a and b in terms of the density operator for mode a alone:

$$W = \left(\rho - \frac{\chi^2}{\gamma^2}X_1\rho X_1\right)\otimes|0\rangle_b\langle 0| + \left(\frac{-i\chi}{\gamma}X_1\rho\otimes|1\rangle_b\langle 0| + \mathrm{H.c.}\right) + \frac{\chi^2}{\gamma^2}X_1\rho X_1\otimes|1\rangle_b\langle 1| + \left(\frac{-\chi^2}{\sqrt{2}\gamma^2}X_1^2\rho\otimes|2\rangle_b\langle 0| + \mathrm{H.c.}\right). \tag{3.22}$$

Now from Sec. II, the result of a photodetection in the output field of mode b is determined by the superoperator $\mathcal{J}$, defined by

$$\mathcal{J}W = \gamma bWb^\dagger. \tag{3.23}$$

To determine the effect of this on mode a, we trace over mode b using (3.22) to find

$$\mathrm{Tr}_b(\mathcal{J}W) = \frac{\chi^2}{\gamma}X_1\rho X_1 = \mathcal{J}_a\rho. \tag{3.24}$$

Similarly we find

$$\mathrm{Tr}_b[(\mathcal{L}-\mathcal{J})W] = \mathrm{Tr}_b\left[\mathcal{L}_0 W - \frac{i\chi}{2}[X_1 Y_1, W] - \frac{\gamma}{2}(b^\dagger b W + W b^\dagger b)\right] = \mathcal{L}_0\rho - \frac{\chi^2}{2\gamma}(X_1^2\rho + \rho X_1^2) = (\mathcal{L}_a - \mathcal{J}_a)\rho. \tag{3.25}$$

Thus we have established that, under the adiabatic assumption behind master equation (3.13), a quantum trajectory of mode a based on the history of photodetections from mode b is identical to a quantum trajectory based on a direct "unraveling" of that master equation as in (3.16). This establishes the physical significance of a state vector (or density matrix) conditional on the history of collapses via $\mathcal{J}_a$.

C. Long counting-time results

1. Photon-counting statistics

From the theory in Sec. II, it is evident that the probability for the photodetector to count m photons in the time t is

$$P_m(t) = \mathrm{Tr}\left[\int_0^t dt_m \int_0^{t_m} dt_{m-1} \cdots \int_0^{t_2} dt_1\, \mathcal{S}_a(t-t_m)\mathcal{J}_a\mathcal{S}_a(t_m - t_{m-1})\cdots\mathcal{J}_a\mathcal{S}_a(t_1)\rho(0)\right]. \tag{3.26}$$

From now on, we ignore the internal dynamics of mode a. Recall that the free (harmonic-oscillator) dynamics were incorporated from the start by working in the interaction picture. Under this assumption, the trace is easy to evaluate in the X_1 representation, which we denote by $X_1|x\rangle = x|x\rangle$,

$$P_m(t) = \frac{(\Gamma t)^m}{m!}\int dx (x^2)^m e^{-\Gamma t x^2} P(x,0), \tag{3.27}$$

where $P(x,0) = \langle x|\rho(0)|x\rangle$. Since both $\mathcal{J}_a$ and $\mathcal{S}_a(t)$ commute with X_1, this result is also proportional to the probability density to detect m photons at any choice of times $t_1, t_2, \ldots, t_m$ between 0 and t. That is, the particular history of counts does not matter, only the tally m by time t.

This probability distribution easily yields the first- and second-order moments,

$$\langle m\rangle = \Gamma t\langle x^2\rangle, \tag{3.28}$$

$$V(m) = (\Gamma t)^2 V(x^2) + \Gamma t\langle x^2\rangle, \tag{3.29}$$

where the averages on the right-hand side of these equations are found from the initial probability distribution for the X_1 quadrature, $P(x,0)$. It is evident from these relations that the QND measurement scheme presented actually measures X_1^2, rather than X_1. This distinction is important because, unlike other observables such as $a^\dagger a$, X_1 has negative eigenvalues, so that the eigenvalues of X_1^2 are degenerate. For long times ($\Gamma t \to \infty$), we have the following result:

$$\langle m\rangle/\sqrt{V(m)} \to \langle x^2\rangle/\sqrt{V(x^2)}. \tag{3.30}$$

Thus, the QND scheme measures X_1^2 arbitrarily accurately.

2. Conditioned system state

The conditional probability distribution for X_1 at time t, given a photon count of m, is evidently given by

$$P_c(x,t)^{(m)} = [P_m(t)]^{-1}\frac{(\Gamma t)^m}{m!}x^{2m}e^{-\Gamma t x^2}P(x,0). \tag{3.31}$$

For long times and correspondingly large m, the function $x^{2m}e^{-\Gamma t x^2}$ is sharply peaked at $x = \pm\sqrt{m/(\Gamma t)}$, with a width which scales as $1/\sqrt{\Gamma t}$. If the variation of $P(x,0)$ across this width may be ignored, then it is possible to obtain simple expressions for the moments of the conditioned distribution $P(x,t)^{(m)}$ as $\Gamma t \to \infty$,

$$\langle x^2\rangle_c^{(m)} = \int dx\, x^{2m+2}e^{-\Gamma t x^2}P(x,0)\left[\int dx\, x^{2m}e^{-\Gamma t x^2}P(x,0)\right]^{-1}$$

$$\to \int_0^\infty dx\, x^{2m+2}e^{-\Gamma t x^2}\left[\int_0^\infty dx\, x^{2m}e^{-\Gamma t x^2}\right]^{-1} = \frac{m+1/2}{\Gamma t}, \tag{3.32}$$

$$V(x^2)_c^{(m)} \to \frac{m+1/2}{(\Gamma t)^2}. \tag{3.33}$$

Since m scales as Γt, the variance of X_1^2 goes to zero for long counting times, leaving the system in an eigenstate of X_1^2 as expected.

As noted above, this does not necessarily mean that the system is left in an eigenstate of X_1. This is because the final probability distribution $P_c(x,t)$ is bimodal, with peaks near $\pm\sqrt{m/(\Gamma t)}$. However, if the initial distribution $P(x,0)$ is localized to the left or right of $x=0$, then the final distribution will be unimodal. In the limit as $\Gamma t, m \to \infty$, we find

$$\langle x\rangle_c^{(m)} \to \pm\sqrt{\frac{m}{\Gamma t}}\left(1+\frac{1}{8m}+\cdots\right), \tag{3.34}$$

$$V(x)_c^{(m)} \to \frac{1}{4\Gamma t} \to 0. \tag{3.35}$$

Thus in this case, the system approaches an eigenstate of X_1 for long periods of counting.

In fact, all of the preceding expressions from (3.27) to (3.35) are valid in the case when the photodetector is not perfect. It is only necessary to replace the previous expression $\Gamma = \chi^2/\gamma$ by $\Gamma = \eta\chi^2/\gamma$, where $\eta \in [0,1]$ is the quantum efficiency of the photodetector. However, it is only in the case $\eta = 1$ that $\mathcal{S}(t)$ may be factorized (3.17), and so preserve pure states. It is to the conditioned pure state of the system under QND quadrature measurement that we now turn.

The generalized Dyson expansion (3.16) is composed of the weighted sum of the (unnormalized) density operator conditioned on the photocount m,

$$\tilde{\rho}_c^{(m)}(t) = \mathcal{S}_a(t)\mathcal{J}^m\rho(0). \tag{3.36}$$

This expression is as simple as it is because $\mathcal{S}_a(t)$ and $\mathcal{J}_a$ commute. Since $\mathcal{S}_a$ can be factorized as in (3.17), with $N(t) = \exp(-\Gamma t X_1^2/2)$, the conditioned density operator can also be factorized, providing that it is initially in a pure state. This gives the following expression for the unnormalized conditioned wave function in the X_1 representation:

$$\tilde{\psi}_c^{(m)}(x,t) = x^m e^{-\Gamma t x^2/2}\psi(x,0). \tag{3.37}$$

From the preceding results, in the long-time limit, the function $x^m e^{-\Gamma t x^2/2}$ becomes sharply peaked at $x = \pm\xi$, where we have defined $\xi = \sqrt{m/\Gamma t}$. As $\Gamma t, m \to \infty$, the function can be approximated by two narrow Gaussians, of variance $(2\Gamma t)^{-1}$. This gives the following asymptotic expression for the conditioned wave function:

$$\psi_c^{(m)}(x,t) \to \left(\frac{\Gamma t}{\pi}\right)^{1/4} \frac{(-1)^m e^{-\Gamma t(x+\xi)^2}\psi(-\xi,0) + e^{-\Gamma t(x-\xi)^2}\psi(\xi,0)}{\left[|\psi(-\xi,0)|^2 + |\psi(\xi,0)|^2\right]^{1/2}}. \tag{3.38}$$

If $m = 0$, which has vanishing probability as $\Gamma t \to \infty$, then the preceding expression is invalid, and we have instead

$$\psi_c^{(0)}(x,t) \to \left(\frac{\Gamma t}{2\pi}\right)^{1/4} \frac{e^{-\Gamma t x^2/2}\psi(0,0)}{|\psi(0,0)|}. \tag{3.39}$$

Evidently, (3.38) represents a coherent superposition of two near eigenstates of the X_1 quadrature operator. There is no apparent reason why such a superposition could not be macroscopic. However, as noted above, this would not occur if the initial state of the field were localized in the X_1 representation. In that case either $\psi(\xi,0)$ or $\psi(-\xi,0)$ could be ignored and the system would evolve towards an eigenstate of X_1. The Husimi function $Q(\alpha) = \langle\alpha|\rho|\alpha\rangle$ for such a state is given as

$$Q(a+ib) \simeq \frac{2}{(\Gamma t)^2}\exp[-2(a\pm\xi)^2]\exp[-2b^2(\Gamma t)^{-4}]. \tag{3.40}$$

This clearly shows that the variance in the conjugate observable X_2 is driven to infinity by a perfect ($\Gamma t \to \infty$) QND measurement of X_1. In Fig. 2 we show the Q function for the cavity mode at various times conditioned on typical QND-measurement results. Here, the initial condition is a Fock state $n = 8$, which is not localized in X_1 space. Hence the collapse of the state towards an eigenstate of X_1^2, rather than of X_1, is evident.

IV. HOMODYNE MEASUREMENT

The theory presented in this section is essentially that of Carmichael [8], made more rigorous and extended. In particular, we demonstrate that the theory is self-consistent, generalize it for imperfect photodetectors, and prove that it reproduces the standard expression for the homodyne photocurrent two-time autocorrelation function. In considering the conditioned state of the system, we examine nonstationary homodyne measurements on a bare cavity field. From this, a number of analytical results are obtained, the most important of which is that homodyne measurements cannot produce a nonclassical (e.g., squeezed) state. Numerical results are also presented.

A. Stochastic evolution under homodyne measurement

1. Discrete homodyne detections

Consider the model of simple homodyne measurement (SHM) shown in Fig. 3. For simplicity, we consider a single-mode cavity of linewidth γ with no internal dynamics. The density operator for this mode a obeys the master equation

$$\dot{\rho} = \frac{\gamma}{2}(2a\rho a^\dagger - a^\dagger a\rho - \rho a^\dagger a). \tag{4.1}$$

The output field from this mode and a local oscillator are incident on a beam splitter. The local oscillator is treated as a classical coherent state with photon flux $\gamma|\alpha|^2$. The transmittivity of the beam splitter with respect to the cavity output field is η. The transmitted field incident on the photodetector, ignoring vacuum fluctuations, is [13]

$$C = \sqrt{\gamma}\left(\sqrt{\eta}\,a + i\sqrt{1-\eta}\,\alpha\right). \tag{4.2}$$

We assume that $\eta \to 1$ and $|\alpha| \to \infty$ such that $\beta = i\sqrt{1-\eta}\,\alpha$ remains finite. Thus the detected field becomes

$$C = \sqrt{\gamma}\,(a+\beta). \tag{4.3}$$

In order to measure the X_1 quadrature of mode a, we wish to have β real, and later we will also assume that β is suitably large.

Note that the field in (4.3) differs from that in simple

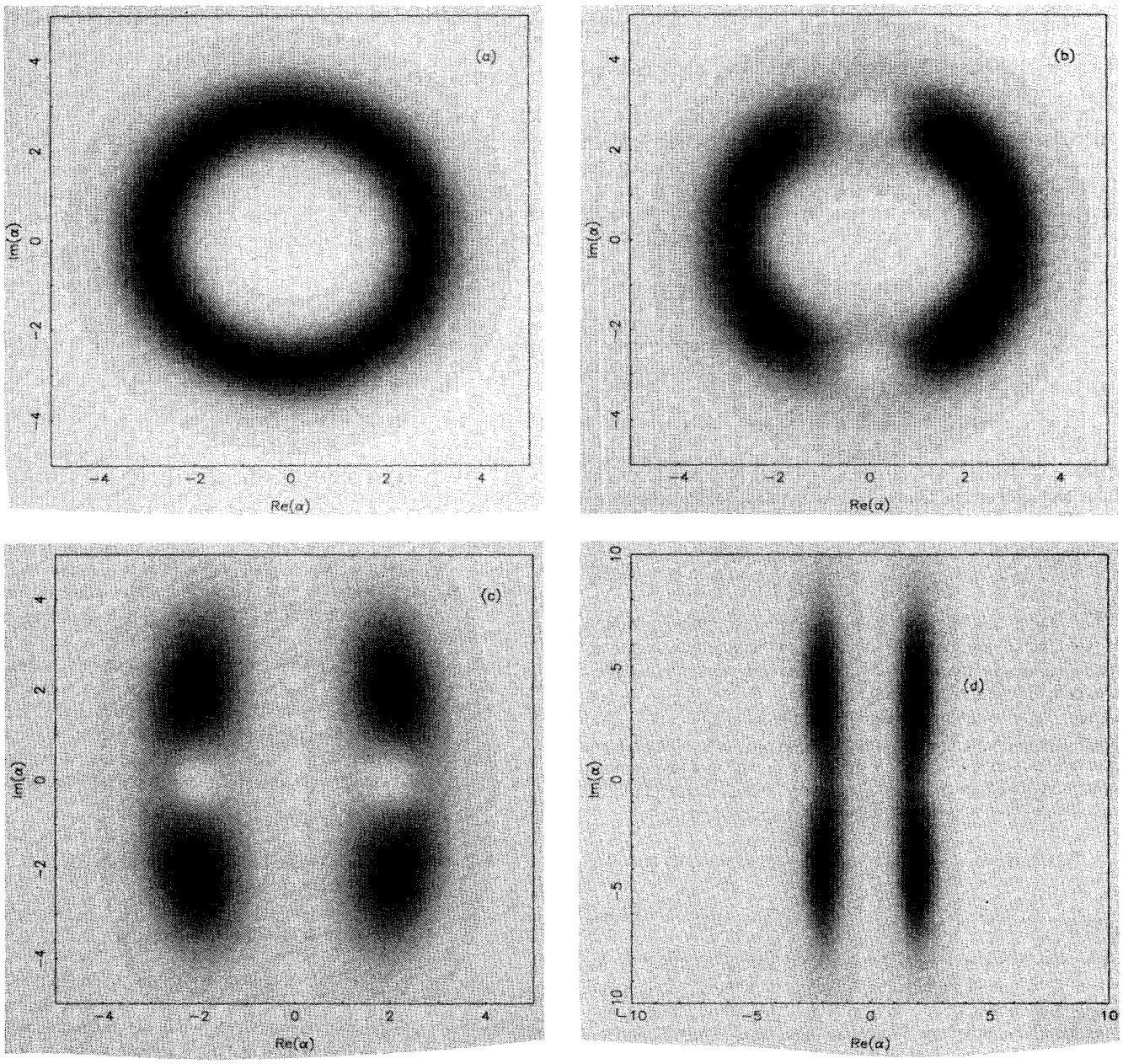

FIG. 2. Gray-scale plot of the Q function for the a mode conditioned on typical QND-measurement results. Initially (a) the system is in a Fock state $n = 8$. (b) shows the state at time $t = 0.25$ and photoncount $m = 1$; (c) at $t = 3.0$ and $m = 12$; and (d) at $t = 30$ and $m = 120$. Time is measured in inverse units of the measurement rate Γ.

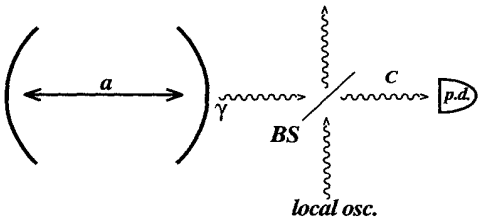

FIG. 3. Schematic diagram of simple homodyne detection. The beam splitter of transmittivity $\eta \to 1$ is denoted by BS and the photodetector by p.d.

photodetection (2.4) only by an additive constant. This means that we can define the superoperator describing the change in the system state when a photodetection occurs by $\mathcal{J}\rho = C\rho C^\dagger$ as before, and rewrite the master equation (4.1) as

$$\dot{\rho} = \mathcal{J}\rho - \frac{\gamma}{2}[(a^\dagger a + 2\beta a + \beta^2)\rho + \rho(a^\dagger a + 2\beta a^\dagger + \beta^2)]. \tag{4.4}$$

One thus obtains a smooth evolution operator $\mathcal{S}(t) = e^{(\mathcal{L}-\mathcal{J})t}$ which preserves pure states, being of the form $\mathcal{S}(t)\rho = N(t)\rho N(t)^\dagger$, where

$$N(t) = \exp\left[-\frac{\gamma}{2}(a^\dagger a + 2\beta a + \beta^2)t\right]. \tag{4.5}$$

Given the operators (4.3) and (4.5) it is possible to simulate SHM by the method outlined in Sec. II, Eqs. (2.15)–(2.17). For example, the collapse probability per unit time is

$$p_c = \langle C^\dagger(t)C(t)\rangle_c = \gamma\langle\psi_c(t)|\beta^2 + 2\beta X_1 + a^\dagger a|\psi_c(t)\rangle, \tag{4.6}$$

where $|\psi_c(t)\rangle$ is the conditioned state of the a mode given the photodetection history up to time t, and $X_1 = (a + a^\dagger)/2$ as in Sec. III. If we make

$$\frac{\langle a^\dagger a\rangle_c}{\beta\langle X_1\rangle_c} \sim \epsilon \ll 1, \tag{4.7}$$

and ignore the constant term in (4.6), then we get a rate of photodetections proportional to $X_1 + O(\epsilon)$, as expected.

However, there are a number of faults with this scheme. Firstly, the photon flux in this case is of the order β^2 times as large as that in standard photon counting (Sec. II). This means that in order to keep the collapse probability per step small in numerical simulations, it would be necessary to reduce the time step and hence increase the simulation time by the same order. Yet any simulation with β finite is in some sense less than ideal. There is another conceptual disadvantage that, since the local oscillator is treated classically, it would be natural for the measured quantity to be represented classically as a photocurrent rather than as discrete photodetections. We thus seek a continuous evolution equation for $|\psi_c(t)\rangle$, valid in the limit $\beta \to \infty$, which would eliminate these demerits. The method we present below is a rigorous reworking of that sketched by Carmichael [8].

2. *Continuous homodyne measurement*

Consider the evolution of the system over the short-time interval $[0, \Delta t]$ where

$$\gamma\Delta t \sim \epsilon^{3/2} \ll 1. \tag{4.8}$$

We link the scaling of Δt to that of $\beta \sim \epsilon^{-1} \gg 1$ so that (i) there are many photodetections ($\beta^2\gamma\Delta t \sim m \sim \epsilon^{-1/2}$), eventually allowing the photocount to be replaced by a photocurrent, but (ii) the change in the system is infinitesimal ($\beta^2\epsilon\gamma\Delta t \sim \epsilon^{1/2} \ll 1$), allowing a differential equation to be derived. From the theory in Sec. II, the probability distribution for the number of photodetections in the time interval is given by

$$P_m(\Delta t) = \mathrm{Tr}\left[\int_0^{\Delta t} dt_m \int_0^{t_m} dt_{m-1} \cdots \int_0^{t_2} dt_1\, \mathcal{S}(\Delta t - t_m)\mathcal{J}\mathcal{S}(t_m - t_{m-1})\cdots\mathcal{J}\mathcal{S}(t_1)\rho(0)\right], \tag{4.9}$$

where $\mathcal{S}(t)$ and $\mathcal{J}$ are as defined immediately above. It is shown in Appendix A that this probability distribution is consistent with a Gaussian of mean

$$\bar{m} = \gamma\Delta t[\beta^2 + 2\beta\langle X_1\rangle(0)] + O(\epsilon) \tag{4.10}$$

and variance

$$\sigma^2(m) = \gamma\Delta t\beta^2 + O(1), \tag{4.11}$$

where $\langle X_1\rangle(0) = \langle\psi(0)|X_1|\psi(0)\rangle$. These results are not surprising, given the instantaneous count rate (4.6) and the dominance of the Poisson statistics of the local oscillator. They allow us to approximate the discrete m by a continuous Gaussian random variable,

$$m = \gamma\Delta t\beta^2[1 + 2\langle X_1\rangle/\beta + O(\epsilon^{3/2})] + \sqrt{\gamma}\Delta W\beta[1 + O(\epsilon^{1/2})]. \tag{4.12}$$

Here, ΔW is a Weiner increment [14] satisfying $\langle(\Delta W)^2\rangle_E = \Delta t$, where the subscript E denotes an ensemble average.

The conditioned state of the system at time Δt will depend on the number of photodetections m, and the times at which those detections occur, $t_1, \ldots, t_m \in [0, \Delta t]$:

$$|\tilde{\psi}_c(\Delta t)\rangle = N(\Delta t - t_m)CN(t_m - t_{m-1})\cdots CN(t_1)|\psi_c(0)\rangle, \tag{4.13}$$

where C and $N(t)$ are the operators defined in (4.3) and (4.5), respectively. Recall that the tilde denotes an unnormalized state. It is shown below that, for the time scale of interest, this conditioned state is independent of the photodetection times $t_1, ..., t_m$, up to $O(\epsilon^{3/2})$. This allows one to move all of the collapse operators C to the front of (4.13), and use the composition property of $N(t)$ to write

$$|\tilde{\psi}_c(\Delta t)\rangle \simeq N(\Delta t)C^m|\psi_c(0)\rangle \tag{4.14}$$

$$\simeq \exp\left[-\frac{\gamma}{2}(2\beta a + a^\dagger a)\Delta t\right]\left(1+\frac{a}{\beta}\right)^m|\psi_c(0)\rangle. \tag{4.15}$$

Note that we have removed a factor of $(\sqrt{\gamma}\beta)^m \exp(-\gamma\beta^2\Delta t/2)$ in going from (4.14) to (4.15). This ensures that the unnormalized conditioned state $|\tilde{\psi}_c(\Delta t)\rangle \to |\psi(0)\rangle$ as $\Delta t \to 0$. We can thus write the following expression for the increment in the system ket:

$$\begin{aligned}\Delta^{(m)}|\tilde{\psi}\rangle &= |\tilde{\psi}_c(\Delta t)\rangle - |\psi(0)\rangle \\ &= \left\{\left[(m-\mu)\frac{a}{\beta}\right] + \left[\left(\frac{\mu^2}{2} + \frac{m(m-1)}{2} - m\mu\right)\left(\frac{a}{\beta}\right)^2\right]\right. \\ &\quad \left. + \left[-\mu\beta^{-2}\frac{a^\dagger a}{2} + \left(-\frac{\mu^3}{6} + \frac{\mu^2 m}{2} - \frac{\mu m(m-1)}{2} + \frac{m(m-1)(m-2)}{6}\right)\left(\frac{a}{\beta}\right)^3\right] + O(\epsilon^2)\right\}|\psi(0)\rangle,\end{aligned} \tag{4.16}$$

where we have used μ as an abbreviation for $\gamma\Delta t\beta^2$. The three terms enclosed in large square brackets are of order $\epsilon^{1/2}$, ϵ, and $\epsilon^{3/2}$, respectively. This expression is precisely the same as that which would have been obtained if all of the collapse operators C had been moved to the rear of (4.13), rather than the front. This is the proof of the earlier claim that the conditioned state is independent of the photodetection times up to order $\epsilon^{3/2}$.

Now, we can substitute expression (4.12) for m into (4.16) to obtain a stochastic increment. Since the ensemble average of ΔW is zero, but that of $(\Delta W)^2$ is Δt, we treat $\sqrt{\gamma}\Delta W$ as if it were of order $\gamma\Delta t \sim \epsilon^{1/2}$. Keeping terms up to order $\epsilon^{3/2}$ as before gives the following:

$$\Delta|\tilde{\psi}\rangle = \left[\gamma\Delta t\left(2\langle X_1\rangle_c a - \frac{a^\dagger a}{2} - \frac{a^2}{2}\right) + \gamma(\Delta W)^2\frac{a^2}{2} + \sqrt{\gamma}\Delta W\, a\right]|\psi(0)\rangle. \tag{4.17}$$

Recall that the averages are evaluated using $|\psi(0)\rangle$, the state of the system at the start of the time increment (conditioned on the stochastic results of all previous increments). If we now let $\beta \to \infty$, then $\epsilon \to 0$ and we can take the continuum limit, making the replacements $\Delta t \to dt$, and $\Delta W \to dW$. Here $dW(t)$ is to be interpreted in terms of Ito stochastic differential equations [14]. Terms of order dW are to be regarded as the same order as dt, but $dW^2 = dt$. These results produce the following stochastic evolution equation for the system ket:

$$|\tilde{\psi}_c(t+dt)\rangle = \left\{1 - \frac{\gamma}{2}dt a^\dagger a + [\gamma dt 2\langle X_1(t)\rangle_c + \sqrt{\gamma}dW(t)]\, a\right\}|\psi_c(t)\rangle. \tag{4.18}$$

This is the expression obtained by Carmichael [8]. For simulations, the infinitesimally evolved state must be normalized at each time step in order to obtain the new averages. The explicit incorporation of this normalization is treated in Sec. IV B 1.

The system ket at a given time, generated by Eq. (4.18), may be interpreted as the conditioned state of the system given the results of the homodyne detection up to that time. Recall that the photon count in a short time (compared to the time scale of change of the system) is approximated by (4.12). In the limit $\beta \to \infty$, this continuous random variable represents the photocurrent. Making this transition was a primary motivation for developing this theory. Subtracting the background photocurrent due to the local oscillator gives a signal photocurrent of

$$I_c(t) = \beta[2\gamma\langle X_1(t)\rangle_c + \sqrt{\gamma}\xi(t)], \tag{4.19}$$

where $\xi(t) = dW(t)/dt$ represents Gaussian white noise. Thus, the homodyne photocurrent is completely determined (within a multiplicative constant) by the conditional evolution of the system, and vice versa.

B. Consistency with previous results

1. *Reproducing the original master equation*

The homodyne measurement of the output field from a cavity does not directly interfere with the internal dynamics of the cavity. Thus, an average of a large ensemble of quantum trajectories generated as described in Sec. IV A 2 should reproduce the same evolution of the cavity mode as would be found by any other means. In quantum mechanics, ensembles are conventionally

treated using density operators. The ensemble average evolution of the density operator should thus reproduce the original master equation (4.1) describing a decaying cavity mode.

From (4.18), we have

$$\begin{aligned}\tilde{\rho}_c(t+dt) &= |\tilde{\psi}_c(t+dt)\rangle\langle\tilde{\psi}_c(t+dt)| \\ &= \rho_c + \frac{\gamma}{2}(2a\rho_c a^\dagger dW^2 - a^\dagger a\rho_c dt - \rho_c a^\dagger a dt) \\ &\quad + [\langle a+a^\dagger\rangle_c \gamma dt + \sqrt{\gamma}dW(t)](a\rho_c + \rho_c a^\dagger),\end{aligned} \tag{4.20}$$

where the conditional averages are evaluated at time t using $\rho_c \equiv \rho_c(t) = |\psi_c(t)\rangle\langle\psi_c(t)|$. Now to normalize this conditional density operator we divide by the trace

$$\mathrm{Tr}[\tilde{\rho}_c(t+dt)] = 1 + [\langle a+a^\dagger\rangle_c \gamma dt + \sqrt{\gamma}dW(t)]\langle a+a^\dagger\rangle_c. \tag{4.21}$$

Expanding this denominator and using the rules of Ito stochastic differential calculus [14] yields

$$\begin{aligned}\rho_c(t+dt) = \rho_c &+ \frac{\gamma}{2}dt(2a\rho_c a^\dagger - a^\dagger a\rho_c - \rho_c a^\dagger a) \\ &+ \sqrt{\gamma}dW(t)(a\rho_c + \rho_c a^\dagger - \langle a+a^\dagger\rangle_c \rho_c).\end{aligned} \tag{4.22}$$

This equation is obviously trace preserving, and it is easy to verify that it also preserves idempotency (that is, it transforms pure states into pure states) as expected. In taking the ensemble average, $\langle dW(t)\rangle_E = 0$, so that the last term disappears and one reproduces the standard master equation

$$\begin{aligned}\frac{d}{dt}\langle\rho_c(t)\rangle_E = \frac{\gamma}{2}[\,&2a\langle\rho_c(t)\rangle_E a^\dagger - a^\dagger a\langle\rho_c(t)\rangle_E \\ &- \langle\rho_c(t)\rangle_E a^\dagger a].\end{aligned} \tag{4.23}$$

The stochastic master equation (4.22) has an advantage over the stochastic ket evolution equation in that nonunitary processes can be incorporated directly. In particular, if the detector efficiency (or equivalently, the beam-splitter transmittivity) η is finitely less than one then the photon tally will be likewise reduced. This degradation in the record of the irreversible evolution of the system means that pure states will not be preserved. It is easy to see that the master equation in this case is simply

$$\begin{aligned}\dot{\rho}_c = &\frac{\gamma}{2}(2a\rho_c a^\dagger - a^\dagger a\rho_c - \rho_c a^\dagger a) \\ &+ \sqrt{\gamma\eta}\xi(t)(a\rho_c + \rho_c a^\dagger - \langle a+a^\dagger\rangle_c \rho_c),\end{aligned} \tag{4.24}$$

where $\xi(t)$ is as defined in Sec. IV A. This approach to nonperfect photodetection is different from that suggested by Carmichael [8]. He uses "lax quantum trajectories" (see end of Sec. II) in which the stochastic term in (4.18) is divided into two uncorrelated terms with coefficients $\sqrt{1-\eta}$ and $\sqrt{\eta}$. Only the latter contributes to the photocurrent, so that the simulated ket is conditioned on a virtual homodyne photocurrent, and so cannot be regarded as representing a real conditioned state. In contrast, the density operator in (4.24) does represent such a state.

2. *Photocurrent autocorrelation functions*

The form of the homodyne photocurrent (4.19) from a detector of efficiency η,

$$I_c(t) = \beta[2\gamma\eta\langle X_1(t)\rangle_c + \sqrt{\gamma\eta}\xi(t)], \tag{4.25}$$

is as expected: a deterministic term proportional to the quantum conditioned average of the X_1 quadrature plus a stochastic term representing the shot noise of the local oscillator. However, we have not yet shown that this expression yields the correct autocorrelation functions. To do this is nontrivial, firstly because in (4.25) $X_1(t)$ is usually regarded as a Heisenberg picture operator whereas we are in the Schrödinger (strictly, interaction) picture, and secondly because we have two distinct averages, classical and quantum, which are usually incorporated together in the density operator. In fact, this second difficulty is actually a conceptual advantage because it allows us to define autocorrelation functions as classical ensemble averages, which is what is actually measured experimentally.

The most useful autocorrelation function for the photocurrent is the two-time autocorrelation function defined by

$$R(t;\tau) = \langle I_c(t+\tau), I_c(t)\rangle_E, \tag{4.26}$$

where we are using the notational convention $\langle A, B\rangle = \langle AB\rangle - \langle A\rangle\langle B\rangle$. Substituting the above expression for the photocurrent gives

$$\frac{R(t;\tau)}{\gamma\eta\beta^2} = 4\gamma\eta\langle\langle X_1\rangle_c(t+\tau)\langle X_1\rangle(t)\rangle_E \tag{4.27a}$$

$$+ 2\sqrt{\gamma\eta}\langle\langle X_1\rangle(t)\xi(t+\tau) + \langle X_1\rangle_c(t+\tau)\xi(t)\rangle_E \tag{4.27b}$$

$$+ \langle\xi(t+\tau)\xi(t)\rangle_E \tag{4.27c}$$

$$- 4\gamma\langle\langle X_1\rangle_c(t+\tau)\rangle_E\langle\langle X_1\rangle(t)\rangle_E. \tag{4.27d}$$

We have dropped the conditional subscript on $\langle X_1\rangle(t)$ because this is determined from the state $\rho(t)$ of the system at the start of the interval, and it is irrelevant whether this state is conditioned on prior measurements. However, the quantum average of X_1 at time $t+\tau$ must be a conditioned average, because it is evaluated using the conditioned density operator, which is determined by the noise in the photocurrent in the interval $[t, t+\tau)$. This conditioned density operator satisfies the stochastic master equation (4.24) which can be split into two terms:

$$\dot{\rho}_c = \mathcal{L}\rho_c + \xi(t)\mathcal{H}\rho_c. \tag{4.28}$$

The deterministic, linear evolution is governed by the superoperator

$$\mathcal{L}\rho = \mathcal{L}_0\rho + \frac{\gamma}{2}(2a\rho a^\dagger - a^\dagger a\rho - \rho a^\dagger a), \tag{4.29}$$

where we have added $\mathcal{L}_0$ to describe any internal evolution of the cavity mode. The stochastic term involves a nonlinear superoperator

$$\mathcal{H}\rho = \sqrt{\gamma\eta}[a\rho + \rho a^\dagger - \mathrm{Tr}(a\rho + \rho a^\dagger)\rho]. \tag{4.30}$$

We now examine each term in the above expression

for $R(t;\tau)$. In the first term (4.27a), $\langle X_1\rangle(t)$ is simply a constant determined by $\rho(t)$. That is, it is the same in each element of the ensemble and so can be removed from the ensemble average. But then we see that this term simply cancels the last term (4.27d). The first term in (4.27b) similarly contributes nothing to the ensemble average. However, the second term in (4.27b) does contribute even though it seemingly contains only one stochastic term. This is because, as explained above, the conditioned mean of X_1 is determined by $\xi(s)$ on the interval $[t, t+\tau)$. In particular, the correlation of $\langle X_1\rangle_c(t+\tau)$ with $\xi(t)$ will be nonzero. The derivation of this correlation function is nontrivial, and is placed in Appendix B. The result, which is obtained using the decomposition of the stochastic master equation (4.28), is

$$\langle\langle X_1\rangle_c(t+\tau)\xi(t)\rangle_E = 2\sqrt{\gamma\eta}\big(\mathrm{Tr}\{:X_1 e^{\mathcal{L}\tau}[X_1\rho(t)]:\} - \mathrm{Tr}\{X_1 e^{\mathcal{L}\tau}[\rho(t)]\}\mathrm{Tr}\{X_1\rho(t)\}\big), \tag{4.31}$$

where :: denotes the normal ordering of annihilation and creation operators. Finally, the term (4.27c) is simply equal to $\delta(\tau)$.

Thus we have the following expression for the two-time correlation function for the homodyne photocurrent:

$$R(t;\tau) = \gamma\eta\beta^2\left[4\gamma\eta\langle:X_1(t+\tau), X_1(t):\rangle + \delta(\tau)\right], \tag{4.32}$$

where we have used the quantum regression theorem [14] in reverse to write (4.31) in terms of standard quantum averages of Heisenberg picture operators. This expression is precisely that normally used to define squeezing spectra [13]. Higher-order autocorrelation functions could be obtained in a similar manner. Although the above method may not be the easiest way to derive such expressions, it does have the advantage of being most obviously equivalent to the experimental method. The further advantage of the quantum-trajectory approach to homodyne measurement is that it allows each experimental photocurrent record to be associated uniquely with a state of the cavity mode. It is the general properties of these states that we examine in the next section.

C. Conditioned system state

1. Exact results

A particularly useful representation of the stochastic master equation (4.24) is that using the Glauber-Sudarshan P function [5, 6]. Since the P function exists formally for all states [15], we are entitled to use its formal properties to generate moments, without supposition of positivity or nonsingularity. It is shown in Appendix C that the infinitesimally evolved conditional P function under homodyne measurement is

$$P_c(\alpha, t+dt) = e^{\gamma dt}P_c(\alpha e^{\gamma dt}, t)\{1 + \sqrt{\gamma\eta}dW(t)[(\alpha+\alpha^*) - \langle a+a^\dagger\rangle_c]\}. \tag{4.33}$$

An immediate consequence of this result is that if $P(\alpha)$ is initially positive and nonsingular, then it remains so. That is, homodyne measurement cannot produce a nonclassical state from a classical one. In particular, it cannot produce a quadrature squeezed state (variance of X_1 less than 0.25), and so the projection postulate (which would force the system into an X_1 eigenstate) cannot hold in any limit.

From this evolution equation for the P function, it is possible to derive a number of results for ensemble averages which elucidate the effect of homodyne measurement on a mode. To begin, we show in Appendix C that the conditional average of the X_1 quadrature at time $t+dt$ is

$$\langle X_1\rangle_c(t+dt) = e^{-\gamma dt/2}\langle X_1\rangle_c(t) + 2\sqrt{\gamma\eta}dW(t)u_c(t), \tag{4.34}$$

where we have defined

$$u_c(t) = \langle:X_1^2:\rangle_c(t) - \langle X_1\rangle_c^2(t) = V_c[X_1](t) - \tfrac{1}{4}. \tag{4.35}$$

That is, $u_c(t)$ is the normally ordered conditional variance in X_1, in which vacuum fluctuations are ignored.

Taking the ensemble average of (4.34) gives

$$\frac{d}{dt}\langle\langle X_1\rangle_c(t)\rangle_E = -\frac{\gamma}{2}\langle\langle X_1\rangle_c(t)\rangle_E. \tag{4.36}$$

This is identical to the result which would be obtained from the original master equation for a damped cavity (4.1), as indeed it must be since the ensemble average density operator obeys the same equation (4.23). The same applies to any ensemble average of a conditioned average, for example,

$$\frac{d}{dt}\langle\langle a^\dagger a\rangle_c(t)\rangle_E = -\gamma\langle\langle a^\dagger a\rangle_c(t)\rangle_E. \tag{4.37}$$

Figures 4 and 5 show numerical results obtained using an ensemble of 1000 quantum trajectories via the stochastic evolution equation (4.18) which verify the results (4.36) and (4.37), respectively. The respective initial conditions for Figs. 4 and 5 are a coherent state $\alpha = 2+2i$ and a Fock state $n = 8$.

Although the standard density operator is reproduced from the ensemble average of the states undergoing homodyne measurement, this does not mean that all of the information about the ensemble is contained in this density operator. There is an infinite number of ways in

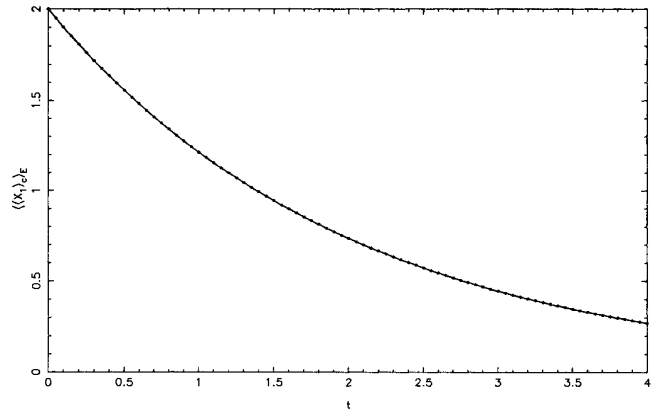

FIG. 4. Plot of the ensemble average (over 1000 quantum trajectories) of the conditional mean of the X_1 quadrature under homodyne measurements for an initial coherent state $\alpha = 2 + 2i$ at regular time intervals. The solid line is the expected exponential decay. Error bars are too small to show. Time is measured in inverse units of the cavity linewidth.

which a nonidempotent density operator can be decomposed into ensembles of nonorthogonal states (the number of which may also be uncountably infinite). Any particular ensemble could represent the collection of conditioned states under some particular measurement scheme (such as homodyne detection, or standard photodetection). We wish to find a quantitative way to differentiate between such ensembles having the same density operator. For a large dimensional Hilbert space, the easiest way is to consider higher-order ensemble averages of conditioned averages. Unlike the first-order moments [such as in Eqs. (4.36) and (4.37)], these may be different in different ensembles. In particular, we will distinguish the homodyne measurement ensemble from the zero-efficiency measurement ensemble whose sole member is the standard density operator.

First, from (4.34) we form

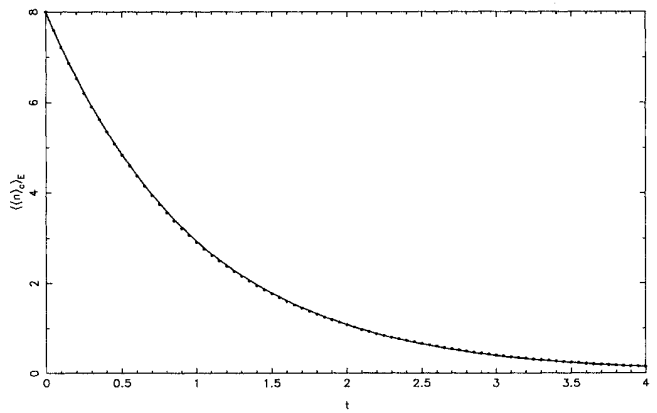

FIG. 5. Plot of the ensemble average of the conditional mean photon number n for an initial Fock state $n = 8$. Other details are as in Fig. 4.

$$\langle X_1\rangle_c^2(t+dt) = e^{-\gamma dt}\langle X_1\rangle_c^2(t) + 4\gamma\eta dt u_c^2(t) + \sqrt{\gamma\eta}dW(t)(\cdots). \tag{4.38}$$

The stochastic term here is unspecified because now we take the ensemble average to get

$$\frac{d}{dt}\langle\langle X_1\rangle_c^2(t)\rangle_E = \gamma[-\langle\langle X_1\rangle_c^2(t)\rangle_E + 4\eta\langle u_c^2(t)\rangle_E]. \tag{4.39}$$

Also from (4.33) we obtain

$$\langle :X_1^2:\rangle_c(t+dt) = \langle :X_1^2:\rangle_c(t)e^{-\gamma dt} + \sqrt{\gamma\eta}dW(t)(\cdots). \tag{4.40}$$

Then, from Eqs. (4.35), (4.38), and (4.40) we get

$$u_c(t+dt) = u_c(t)e^{-\gamma dt} - 4\gamma\eta u_c^2(t)dt + \sqrt{\gamma\eta}dW(t)(\cdots). \tag{4.41}$$

Taking the ensemble average gives

$$\frac{d}{dt}\langle u_c(t)\rangle_E = -\gamma[\langle u_c(t)\rangle_E + 4\eta\langle u_c^2(t)\rangle_E]. \tag{4.42}$$

Some general features of (4.39) and (4.42) are worth noting before proceeding further. If the detector efficiency η goes to zero, then both equations describe the exponential decay predicted by the standard master equation (4.1). The effect of homodyne measurements ($\eta > 0$) on the ensemble mean square of the conditioned average of X_1 is to cause it to increase or slow its rate of decrease. This is expected, as measuring the X_1 quadrature should to some extent force the system into a state with a well-defined X_1 even if initially $\langle X_1\rangle_c = 0$. The effect on the normally ordered variance in X_1 is to decrease it more rapidly (if initially positive) or to make it increase more slowly (if initially negative). Again, this is as expected; measuring X_1 causes the variance in X_1 to be smaller than otherwise.

2. *Approximate results*

At the start of the homodyne measurement, all elements in the ensemble are identical, so $\langle u_c^2(0)\rangle_E = \langle u_c(0)\rangle_E^2$. The factorization approximation (FA), that

$$\frac{|\langle u_c^2(t)\rangle_E - \langle u_c(t)\rangle_E^2|}{\langle u_c^2(t)\rangle_E} \ll 1, \tag{4.43}$$

will be valid for short times providing that $u_c(0)$ is finite. Note, however, that for an initially coherent state [in which $u_c(0) = 0$] the FA will be valid for all times. This is because it will remain a coherent state under homodyne detection [so that $u_c(t) \equiv 0$], which is obvious from the evolution equation for the P function (4.33).

Using this approximation, we can construct a differential equation from (4.42) for $u \equiv \langle u_c\rangle_E$,

$$\frac{d}{dt}u = -\gamma(u + 4\eta u^2). \tag{4.44}$$

This has the solution

$$u(t) = \frac{u_0 e^{-\gamma t}}{1 + 4\eta u_0(1 - e^{-\gamma t})}. \tag{4.45}$$

Clearly this function is monotonic in time, asymptotically approaching zero. If $u_0 \gg 1$, this initially large variance in X_1 is reduced to $(4\eta)^{-1}$, which is of order unity, in one half life of the cavity ($\gamma t = \ln 2$).

In the case when $\eta = 1$ (perfect detection), (4.45) can be more simply expressed in terms of $V = u + \frac{1}{4}$,

$$V(t) = V_0[1 + 4(V_0 - \tfrac{1}{4})(1 - e^{-\gamma t})]^{-1}. \tag{4.46}$$

In Fig. 6 we plot $\sqrt{V(t)}$ determined from an ensemble of 1000 trajectories initially in the Fock state $|8\rangle$. The numerical results agree well with the analytic solution for short times, as expected. However, for longer times, the ensemble mean variance falls below the classical limit of 0.25, a feature which the analytic solution fails to pick up. This indicates the failure of the FA for such times. Thus, although classical states cannot be squeezed by homodyne detection, quadrature squeezing can be typically produced for certain nonclassical (but not quadrature-squeezed) initial states.

Now, using the FA and substituting (4.45) into (4.39) yields

$$\frac{d}{dt}s = \gamma\left(-s + u_0 \frac{4\eta u_0 e^{-2\gamma t}}{[1 + 4\eta u_0(1 - e^{-\gamma t})]^2}\right), \tag{4.47}$$

where we have defined $s \equiv \langle\langle X_1\rangle_c^2\rangle_E$. The solution to this differential equation is

$$s(t) = s_0 e^{-\gamma t} + u_0 e^{-\gamma t}\{1 - [1 + 4\eta u_0(1 - e^{-\gamma t})]^{-1}\}. \tag{4.48}$$

For short times, this solution exhibits linear growth (or inhibited decay if $s_0 > 4\eta u_0^2$),

$$s(t) \simeq s_0 + \gamma t(-s_0 + 4\eta u_0^2), \tag{4.49}$$

while for long times it decays exponentially,

$$s(t) \simeq \left(s_0 + \frac{4\eta u_0^2}{1 + 4\eta u_0}\right) e^{-\gamma t}. \tag{4.50}$$

Numerical results for $\sqrt{s(t)}$, determined as for Fig. 6, are plotted in Fig. 7. They show good agreement with (4.48) for short times, and reasonable agreement well into the exponential decay time regime. The general features of the quantum effects of homodyne measurements thus seem well understood analytically.

Between the two time regimes (4.49) and (4.50), $s(t)$ reaches a maximum at some time t_M, providing $4\eta u_0^2 > s_0$. This time is given by

$$\exp(-\gamma t_M) = 1 + \frac{1}{4\eta u_0}\left[1 - \left(\frac{u_0(1 + 4\eta u_0)}{s_0 + u_0}\right)^{1/2}\right]. \tag{4.51}$$

Substituting into (4.48) gives the maximum value of s to be

$$s_M = \left[1 + 4\eta u_0 - \left(\frac{u_0(1 + 4\eta u_0)}{s_0 + u_0}\right)^{1/2}\right] \times \frac{1}{4\eta}\left[\frac{s_0}{u_0} + 1 - \left(\frac{s_0 + u_0}{u_0(1 + 4\eta u_0)}\right)^{1/2}\right]. \tag{4.52}$$

To elucidate these formulas, we consider the special case $s_0 = 0$; $\eta u_0 \gg 1$. That is, the initial distribution for X_1 has a zero mean and a large variance. This is the situation in which the effect of measuring X_1 will be most dramatic. Examples include a large-n Fock state, or a phase-diffused state such as produced by a laser. We then get

$$\gamma t_M \simeq (4\eta u_0)^{-1/2} \tag{4.53}$$

and

$$s_M \simeq u_0 - (u_0/\eta)^{1/2}. \tag{4.54}$$

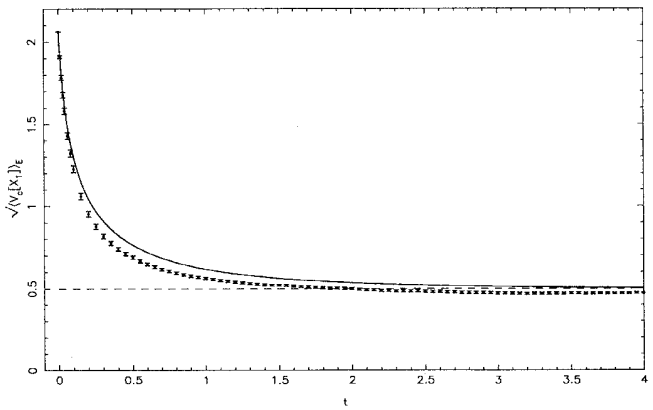

FIG. 6. Plot of the square root of the ensemble average (over 1000 quantum trajectories) of the conditional variance in X_1 under the homodyne measurement for an initial Fock state $n = 8$. The solid line shows an approximate analytic solution, valid for short times. The dashed line indicates the classical limit (uncertainty in X_1 of 0.5). Error bars represent a 95% confidence interval.

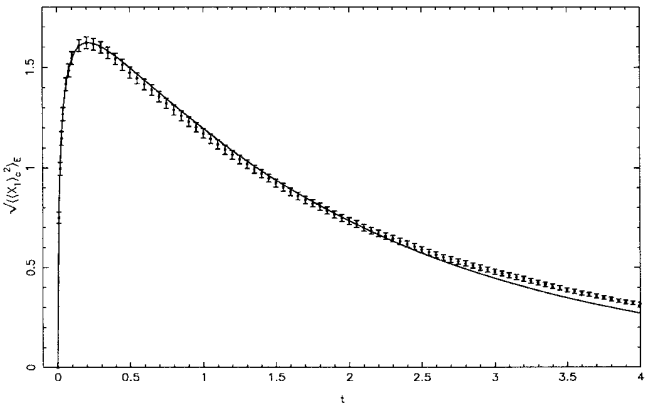

FIG. 7. Plot of the square root of the ensemble average of the square of the conditional mean X_1. Other details are as in Fig. 6.

From (4.45), the normally ordered variance at this time is

$$u(t_M) \simeq (u_0/4\eta)^{1/2}. \tag{4.55}$$

Thus, the initial state in which X_1 is poorly defined is rapidly collapsed into a state with a large mean X_1 (of the order of the initial width of the distribution), and a much smaller uncertainty. Strictly, these formulas (4.51)–(4.55) are not necessarily correct because we have not shown that the FA (4.43) is valid for the time t_M. To do this requires more complete specification of the initial state of the system than is given by s_0 and u_0, and is too detailed to be useful. From the numerical results, the formulas appear valid for a large-n Fock state, and they are not unreasonable in general, illustrating the typical behavior expected.

V. BALANCED HOMODYNE MEASUREMENTS

The theory presented in the previous section was based on simple homodyne detection with only one photodetector. In practice, it is common to use balanced homodyne measurements, with two photodetectors. This gives a much better resolution of X_1 for a given local-oscillator strength. Here we show that it also has advantages for numerical simulations with a finite local oscillator strength. As the strength goes to infinity, BHM gives rise to the same stochastic evolution equation as does SHM.

The model for BHM is shown in Fig. 8. As before, the single mode in the cavity obeys the standard damping master equation (4.1). The transmittivity of the beam splitter is one-half, and the local-oscillator input field is $\sqrt{\gamma}i\beta$, where β is real in order to measure the X_1 quadrature of a. The fields incident on photodetectors D_1 and D_2 are, ignoring vacuum fluctuations,

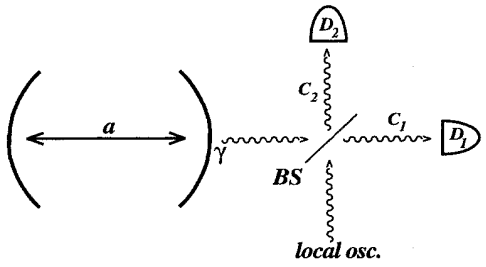

FIG. 8. Schematic diagram of the balanced homodyne detection. The beam splitter (BS) has transmittivity $\frac{1}{2}$. The photodetectors are denoted D_1 and D_2.

$$C_1 = \sqrt{\gamma/2}\,(a-\beta), \tag{5.1}$$

$$C_2 = \sqrt{\gamma/2}\,i(a+\beta), \tag{5.2}$$

respectively. Defining jump superoperators $\mathcal{J}_k\rho = C_k\rho C_k^\dagger$ $(k=1,2)$, we can rewrite the master equation as

$$\dot\rho = \mathcal{J}_1\rho + \mathcal{J}_2\rho - \frac{\gamma}{2}[(a^\dagger a+\beta^2)\rho + \rho(a^\dagger a+\beta^2)]. \tag{5.3}$$

Evidently, the solution of this master equation can be written in terms of generalized Dyson expansions in $\mathcal{J}_2$ nested within the expansion in $\mathcal{J}_1$ (or vice versa),

$$\rho(t) = \sum_{n=0}^{\infty}\int_0^t dt_n \int_0^{t_n} dt_{n-1}\cdots\int_0^{t_2} dt_1\, \mathcal{S}_1(t-t_n)\mathcal{J}_1\mathcal{S}_1(t_n-t_{n-1})\cdots\mathcal{J}_1\mathcal{S}_1(t_1)\rho(0), \tag{5.4}$$

where

$$\mathcal{S}_1(t) = \sum_{m=0}^{\infty}\int_0^t dt_m \int_0^{t_m} dt_{m-1}\cdots\int_0^{t_2} dt_1\, \mathcal{S}(t-t_m)\mathcal{J}_2\mathcal{S}(t_m-t_{m-1})\cdots\mathcal{J}_2\mathcal{S}(t_1) \tag{5.5}$$

describes the smooth evolution of the system given that no photodetections occur at D_1, and averaged over all possible photodetections histories at D_2. When there are no detections at D_2 either, the system evolution is determined by

$$\mathcal{S}(t)\rho = N(t)\rho N(t)^\dagger, \tag{5.6}$$

where

$$N(t) = \exp\left[-\frac{\gamma}{2}(a^\dagger a+\beta^2)t\right]. \tag{5.7}$$

The easiest way to generate such an ensemble of quantum trajectories is via a numerical simulation, which allows information about typical trajectories to be extracted. This could be done in the manner of Sec. II, except with two possible jump processes in each time interval due to photodetections at D_1 and D_2. However, in this case the smooth evolution superoperator (5.6) has such a simple form that the alternative method described below is preferable.

It is easy to see that the probability to detect no photons at either detector in the time interval $[0,t]$, given the initial state $\rho(0)$ of the system, is [1]

$$P_{0,0}(t) = \mathrm{Tr}[\mathcal{S}(t)\rho(0)]. \tag{5.8}$$

If we expand the conditioned system state in the Fock basis as $|\psi(t)\rangle_c = \sum_{n=0}^{\infty} c_n(t)|n\rangle$, then this probability is given by

$$W(t) = \sum_{n=0}^{\infty} e^{-\gamma(n+\beta^2)t}|c_n(0)|^2. \tag{5.9}$$

Here we use the symbol $W(t)$ because it also represents the waiting time distribution to the next photodetection.

Thus, to evolve the system as a quantum trajectory, one first generates a random number r on the unit interval, and from it determines a time

$$t_r = W^{-1}(r), \tag{5.10}$$

where this inverse function is evaluated numerically. Then, the system ket is evolved smoothly forward via

$$|\tilde{\psi}(t_r)\rangle = N(t_r)|\psi(0)\rangle, \tag{5.11}$$

and then normalized. Next, a new random number on the unit interval is generated to determine whether the photodetection which occurs at time t_r is at D_1 or D_2. This choice is made using weights proportional to the probability to detect a photon at D_k,

$$w_k = \langle a^\dagger a + (-1)^k \beta(a + a^\dagger) + \beta^2\rangle(t_r) \propto \langle C_k^\dagger C_k\rangle(t_r). \tag{5.12}$$

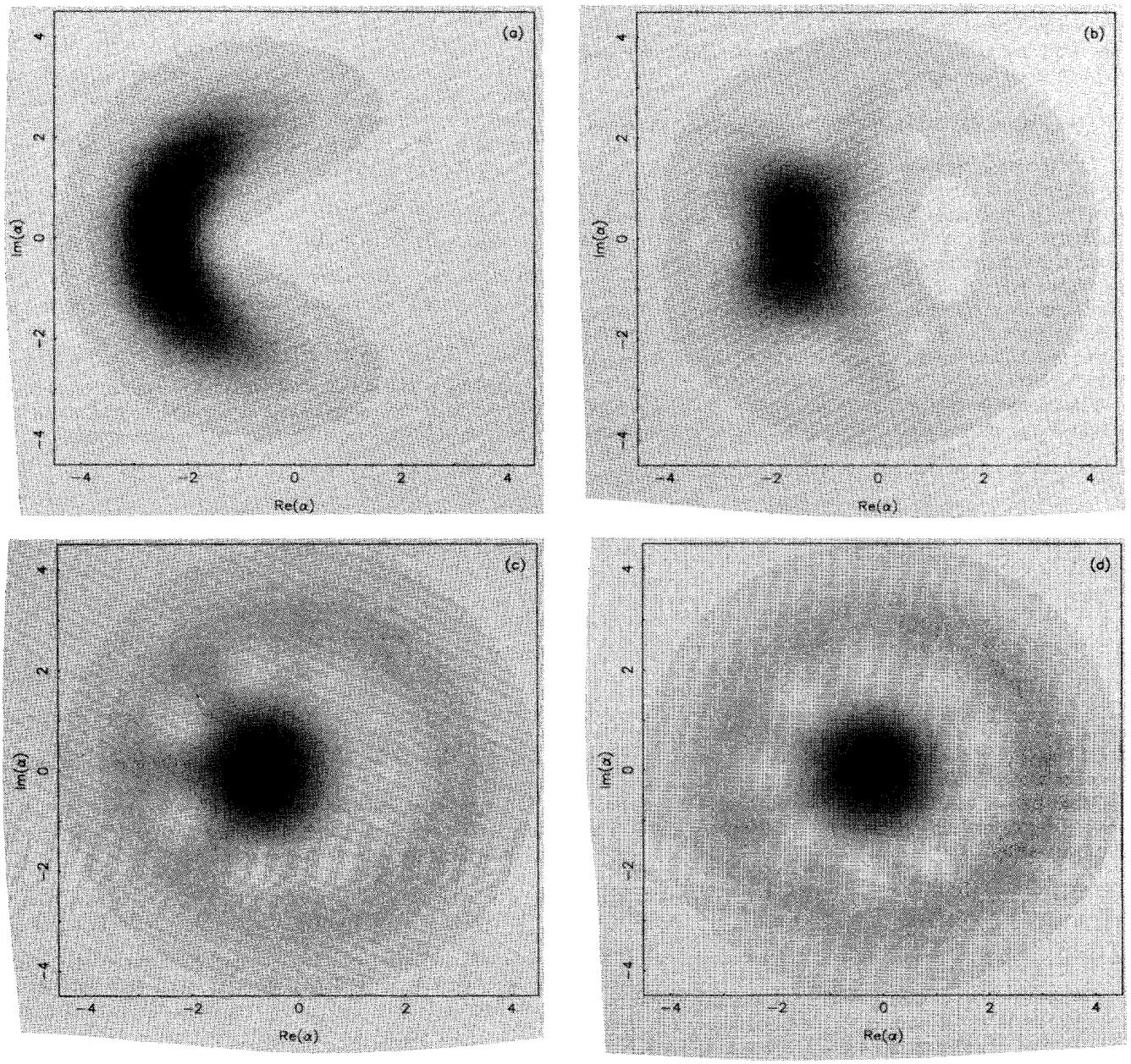

FIG. 9. Gray-scale plot of the Q functions for the cavity mode for a typical quantum trajectory under BHM. Here the initial condition [see Fig. 2(a)] is a Fock state $n = 8$ and the local oscillator is a coherent state $\beta = 100$. The times (measured in inverse units of the cavity linewidth γ) shown are (a) $t = 0.25$, (b) $t = 1.0$, (c) $t = 2.0$, (d) $t = 4.0$. The system at $t = 1.0$ is most squeezed, with an X_1 variance of 0.158.

Once the detector number k has been determined, the new system ket is produced using the appropriate collapse operator

$$|\tilde{\psi}(t_r))' = C_k|\psi(t_r)\rangle, \tag{5.13}$$

and again is normalized.

One of the main results of Sec. IV C 1 was that homodyne measurements maintain the classicality of states. This is easy to establish in the case of balanced homodyne detection, using the above algorithm. From the definition (5.7) of $N(t)$, the P function of a state under smooth nonunitary evolution is

$$P(\alpha,t) = \mathcal{N}P(\alpha e^{-\gamma t/2},0), \tag{5.14}$$

and when a photodetection at D_k occurs, the P function changes to

$$P(\alpha,t)' = \mathcal{N}'|\alpha+(-1)^k\beta|^2P(\alpha,t). \tag{5.15}$$

Here $\mathcal{N}$ and $\mathcal{N}'$ are normalization factors. Obviously both of these processes maintain the positivity of the P function, and so classical states remain classical.

In Fig. 9 we show the Q functions for the cavity mode at various times for a typical quantum trajectory under BHM. Here the initial condition (not shown) is the Fock state $n=8$. This figure is to be contrasted with Fig. 2, which shows the results of the QND measurement scheme for the same initial conditions [shown in Fig. 2(a)]. Here the homodyne measurement does localize the Q function around one value of X_1, but the state is only mildly squeezed and decays to a vacuum for long times. The wealth of fine structure can be interpreted as "quantum phase-space interference." This is not unexpected because all of the states are pure, and the initial state is highly nonclassical.

Because the above method for numerical simulation uses no finite-time step, it may be considerably faster than, for example, the first method described in Sec. IV. However, it suffers from some of the same disadvantages, in that β must be finite. We now show that as $\beta\to\infty$, balanced homodyne detection gives rise to the same stochastic evolution equation as did simple homodyne detection. In fact, the result is somewhat easier to obtain in this case. We proceed rapidly using the same method.

Firstly, we take $\beta\sim\epsilon^{-1}$ large and a short-time interval $\gamma\Delta t\sim\epsilon^{3/2}$. From the method of Appendix A, the photocount of detector D_k in this interval can be written as a stochastic variable

$$m_k = \frac{\gamma}{2}\beta^2[1+(-1)^k2\langle X_1/\beta\rangle_c(t)+O(\epsilon^{3/2})]\Delta t + \sqrt{\frac{\gamma}{2}}\beta[1+O(\epsilon^{1/2})]\Delta W_k, \tag{5.16}$$

where ΔW_k are independent Weiner increments. Now, the unnormalized evolved ket for the system conditioned on the photocounts m_1,m_2 is, with an error of order ϵ^2,

$$|\tilde{\psi}_c(\Delta t)\rangle = \exp\left(-\frac{\gamma}{2}a^\dagger a\Delta t\right)\left(1+\frac{a}{\beta}\right)^{m_2}\left(1-\frac{a}{\beta}\right)^{m_1}\times|\psi(0)\rangle. \tag{5.17}$$

Expanding this to order $\epsilon^{3/2}$ gives the first-order increment in this ket,

$$\Delta^{(m_1,m_2)}|\tilde{\psi}\rangle = \left[-\frac{\gamma}{2}a^\dagger a\Delta t+\frac{a}{\beta}(m_2-m_1)\right]|\psi(0)\rangle, \tag{5.18}$$

where we have used the fact that the difference of the two photocounts is of the order $\epsilon^{1/2}$ to omit higher powers of a/β. Substituting in the stochastic expressions for the photocounts gives, to leading order,

$$\Delta|\tilde{\psi}\rangle = \left\{-\frac{\gamma}{2}a^\dagger a\Delta t+a\left[\gamma 2\langle X_1\rangle_c\Delta t+\sqrt{\frac{\gamma}{2}}(\Delta W_2-\Delta W_1)\right]\right\}|\psi(0)\rangle. \tag{5.19}$$

Taking the continuum limit as $\beta\to\infty$, and defining a new Weiner increment $dW=(dW_2-dW_1)/\sqrt{2}$, gives

$$|\tilde{\psi}_c(t+dt)\rangle = \left\{1-\frac{\gamma}{2}dta^\dagger a+[\gamma dt2\langle X_1(t)\rangle_c+\sqrt{\gamma}dW(t)]\,a\right\}|\psi_c(t)\rangle. \tag{5.20}$$

This is precisely the expression obtained in Sec. IV. In this case, the term in square brackets is proportional to the increment in the difference between the two photocurrents. In BHM this is the signal, so again the evolution of the system is completely determined by the measurement result.

VI. SUMMARY AND APPLICATIONS

The original motivation of this paper was to answer the question, to what extent can homodyne measurements be modeled by the projection postulate? The conclusion is that such measurements of the field quadrature of a cavity mode do not in any limit result in a projective collapse of the state of the mode. Homodyne detection (either simple or balanced) of a nondriven cavity does, as expected for a quantum measurement, cause the conditioned variance in the measured quantity (here the X_1 quadrature) typically to become lower than it otherwise would. However, unless the system is initially in a nonclassical state, the homodyne measurement cannot reduce the variance in X_1 below the classical limit of $\frac{1}{4}$. Thus contrary to expectations, the homodyne measurement does not even produce the squeezed states required

by a finite accuracy projection [4].

This answer should not be regarded as surprising. It was shown some time ago by Srinivas and Davies [1] that standard photodetection (intensity measurement) cannot in any sense be modeled by a projection onto the photon-number eigenstates. In fact, the results obtained here follow on from the theory of standard photodetection of Srinivas and Davies, because the latter is subsumed by Carmichael's theory of quantum trajectories [7, 8], on which the theory in this paper is based. At the heart of this theory of quantum trajectories is the postulate that the operator which represents the field incident on a photodetector outside the cavity is also the operator which transforms the system ket into the new ket conditioned on the detection of a photon at the detector. Thus, the irreversible coupling of the cavity mode to the external continuum of modes is simply and directly incorporated into the theory of quantum trajectories.

The above failure of the projection postulate is a consequence of the method of measurement rather than of the nature of the observed quantity. This point is demonstrated by considering an alternate scheme for measuring X_1 which involves a quantum nondemolition coupling of the X_1 quadrature of the system mode to that of another mode which is part of the apparatus. It is shown that, under appropriate assumptions, this measurement does approach a projective one. (Strictly, the projection is onto eigenstates of X_1^2 rather than X_1, but the distinction is unimportant for suitable initial conditions.) Although this scheme may not be easy, or even feasible, to achieve experimentally, it does indicate that projective measurements are not impossible in principle. Considerable use is made of quantum trajectories in the analysis of this QND scheme also, showing the extension of the theory to more indirect measurements.

The applications of the quantum theory of quadrature measurements are numerous and important. As stated in the Introduction, homodyne measurements have been, in the absence of a correct theory, treated projectively. An example of interest is the localization of atoms by performing a homodyne measurement on the field with which they have interacted, and the subsequent diffraction and interference of the atomic wave function [4]. The effect of realistic (nonprojective) homodyne measurement on the field would be likely to significantly reduce the visibility of the diffraction and interference patterns. If the QND scheme were to be used to measure the field quadrature, the method proposed in Ref. [4] would have to be modified due to the point made parenthetically in the previous paragraph. This matter will be considered in detail elsewhere.

Another issue of interest which could be addressed by the theory presented in this paper is, to what extent can the output of a standard laser monitored by homodyne detection be modeled by a coherent state? In this case, it may be of interest to consider monitoring both quadratures simultaneously, and the theory is easily modified to incorporate this. Preliminary analytical work suggests that the answer to this question on laser output is also negative. The relationship between the laser linewidth, as measured by spectral analysis, and phase diffusion, as measured by homodyne detection, could also be investigated.

Since completing this work we have become aware of other approaches to the simulation of the evolution of open quantum systems using state vectors rather than density matrices [16–19]. As this seems to be an area of considerable current interest we have added Appendix D in order to compare these theories with that presented in this paper. Our conclusion is that the alternate theories, at least in their present formulation, would not allow the derivation of the quantum theory of quadrature measurements presented in this paper. It is only in Carmichael's approach that the state vector used in a simulation can be regarded as a representation of the actual state of the system. The key to this is, as noted above, the identification of the photodetection collapse operator with the operator of the field incident on the photodetector.

Note added: It has been brought to our attention that there exist other approaches to stochastic state-vector evolution [20–22] in addition to those we have discussed here. These include diffusion processes for state vectors, similar to the homodyne ket evolution equation (4.18). However, these models are motivated by abstract measurement theory (dynamical state-vector reduction) rather than by an analysis of realistic measurement schemes. The interpretation of these models, and the others mentioned in Appendix D, will be considered more fully in a forthcoming paper.

APPENDIX A: APPROXIMATION OF THE HOMODYNE PHOTOCOUNT BY A GAUSSIAN RANDOM VARIABLE

From Eq. (4.9) we have the following expression for the probability distribution for the homodyne photocount in the time interval $[0, \Delta t]$:

$$P_m(\Delta t) = \mathrm{Tr}\left[\int_0^{\Delta t} dt_m \int_0^{t_m} dt_{m-1} \cdots \int_0^{t_2} dt_1 \, \mathcal{S}(\Delta t - t_m)\mathcal{J}\mathcal{S}(t_m - t_{m-1}) \cdots \mathcal{J}\mathcal{S}(t_1)\rho(0)\right], \tag{A1}$$

where $\mathcal{J}\rho = C\rho C^\dagger$ and $\mathcal{S}(t)\rho = N(t)\rho N(t)^\dagger$, where

$$C = \sqrt{\gamma}(a + \beta), \quad N(t) = \exp\left[-\frac{\gamma}{2}(\beta^2 + 2\beta a + a^\dagger a)t\right]. \tag{A2}$$

Recall that the local-oscillator amplitude and the time interval are scaled together by

$$\beta \sim \epsilon^{-1}, \quad \gamma \Delta t \sim \epsilon^{3/2}, \tag{A3}$$

where ϵ is a small parameter. This ensures that the number of photodetections, which we scale as

$$\mu \equiv \gamma \Delta t \beta^2 \sim \epsilon^{-1/2}, \tag{A4}$$

is large, while the change in the system is of order $\gamma \Delta t \beta X_1 \sim \epsilon^{1/2}$, which is small. This latter fact allows the $\mathcal{J}$'s and $\mathcal{S}(t)$'s in Eq. (A1) to be commuted with an error of order ϵ^2 (see Sec. IV A). Then the nested time integrals are trivially evaluated to give

$$P_m(\Delta t) = \frac{(\Delta t)^m}{m!} \mathrm{Tr}[\mathcal{S}(\Delta t)\mathcal{J}^m \rho(0)]. \tag{A5}$$

Expanding the above expressions for $\mathcal{J}$ and $\mathcal{S}(\Delta t)$ to first order in ϵ gives

$$P_m(\Delta t) = e^{-\mu}\frac{\mu^m}{m!}\mathrm{Tr}\{[1 + m(a+a^\dagger)/\beta - \gamma \Delta t \beta (a+a^\dagger) + O(\gamma \Delta t) + O(m^2-\mu^2)\beta^{-2}]\rho(0)\}. \tag{A6}$$

This distribution is obviously a small correction to the Poissonian distribution of mean μ which is due to the local oscillator. Hence, we have $O(m^2-\mu^2) = O(\mu)$, and so the last term in the above expansion is of the same order as the second last term, namely $O(\epsilon^{3/2})$. Both may be ignored compared to the leading correction which is of order ϵ. Thus we have the following expression for the probability distribution for m:

$$P_m(\Delta t) = e^{-\mu}\frac{\mu^m}{m!}[1 + (m-\mu)2x\beta^{-1} + O(\epsilon^{3/2})], \tag{A7}$$

where x stands for the quantum average $\mathrm{Tr}[X_1\rho(0)]$.

It is easy to evaluate the moments of this distribution. We find

$$\langle m \rangle = \mu[1 + 2x\beta^{-1} + O(\epsilon^{3/2})], \tag{A8}$$

$$V(m) = \mu[1 + O(\epsilon)], \tag{A9}$$

while higher-order moments ($n > 2$) are given by

$$\langle m^n \rangle - \langle m \rangle^n = \frac{n(n-1)}{2}\mu^{n-1} + \left\{\frac{n(n-1)(n-2)}{6}\mu^{n-2}\right\} + [O(x\beta^{-1}\mu^{n-1}) + O(\mu^{n-3})]. \tag{A10}$$

Recall that $\beta \sim \epsilon^{-1} \sim \mu^2$. Now, we claim that these moments are consistent with those of a Gaussian distribution with mean and variance given by

$$\bar{m} = \mu[1 + 2x\beta^{-1} + O(\epsilon^{3/2})], \tag{A11}$$

$$\sigma^2 = \mu[1 + O(\epsilon^{1/2})]. \tag{A12}$$

The two means (A11) and (A8) are equal, and the two variances (A12) and (A9) are also equal to within the larger uncertainty postulated in σ^2. The higher-order Gaussian moments are given by

$$\langle m^n \rangle_G - \bar{m}^n = \frac{n(n-1)}{2}\bar{m}^{n-2}\sigma^2 + \frac{n(n-1)(n-2)(n-3)}{8}\bar{m}^{n-4}\sigma^4 + O(\bar{m}^{n-6}\sigma^6)$$
$$= \frac{n(n-1)}{2}\mu^{n-2}[\mu + O(1)] + \left\{\frac{n(n-1)(n-2)(n-3)}{8}\mu^{n-2}\right\} + [O(x\beta^{-1}\mu^{n-1}) + O(\mu^{n-3})] \tag{A13}$$

$$= \frac{n(n-1)}{2}\mu^{n-1} + O(\mu^{n-2}). \tag{A14}$$

We see here why it was necessary to introduce a larger uncertainty in σ^2 than the true expression for $V(m)$ (A9) would have suggested: to make the term of order μ^{n-2} in (A14) uncertain. If the uncertainty had been chosen to be the same as that in $V(m)$, then the term of order μ^{n-2} for the nth-order Gaussian moment [in large curly brackets in (A13)] would have disagreed with the corresponding term for the true distribution [in large curly brackets in (A10)]. With the uncertainty in σ^2 as stated (A12), the moments for the two distributions do agree and hence it is valid to approximate the photon-count distribution (A7) by the Gaussian distribution defined by Eqs. (A11) and (A12).

APPENDIX B: DERIVATION OF EQ. (4.31)

We wish to determine the correlation function

$$F(t;\tau) = \langle \langle X_1 \rangle_c (t+\tau)\xi(t)\rangle_E, \tag{B1}$$

where ξ represents δ-function correlated shot noise. This can be rewritten in terms of the conditioned density operator ρ_c as

$$F(t;\tau) = \mathrm{Tr}[X_1 \langle \rho_c(t+\tau)\xi(t)\rangle_E]. \tag{B2}$$

As stated in the text, ρ_c satisfies the following stochastic master equation:

$$\dot{\rho}_c = \mathcal{L}\rho_c + \xi(t)\mathcal{H}\rho_c, \tag{B3}$$

where

$$\mathcal{L}\rho = \mathcal{L}_0\rho + \frac{\gamma}{2}(2a\rho a^\dagger - a^\dagger a\rho - \rho a^\dagger a) \tag{B4}$$

and

$$\mathcal{H}\rho = \sqrt{\gamma\eta}[a\rho + \rho a^\dagger - \mathrm{Tr}(a\rho + \rho a^\dagger)\rho]. \tag{B5}$$

The formal solution to this stochastic differential equation is

$$\rho_c(t+\tau) = T\left\{\exp\left[\mathcal{L}\tau + \int_t^{t+\tau} ds\xi(s)\mathcal{H}\right]\rho(t)\right\}, \tag{B6}$$

where T denotes time ordering. This can be written more explicitly as

$$\rho_c(t+\tau) = \mathcal{R}(t,t+\tau)\rho(t), \tag{B7}$$

where $\mathcal{R}$ is a superoperator defined recursively by

$$\mathcal{R}(t,t+\tau)\rho = e^{\mathcal{L}\tau}\rho + \int_t^{t+\tau} dt_1 e^{\mathcal{L}(t+\tau-t_1)}\xi(t_1)\mathcal{H}[\mathcal{R}(t,t_1)\rho], \tag{B8}$$

where ρ is arbitrary. Since $\xi(t) = dW(t)/dt$, we can rewrite this expansion in terms of Ito stochastic integrals [14]. Using the recursive formula a few times gives

$$\rho_c(t+\tau) = e^{\mathcal{L}\tau}\rho(t) + \int_t^{t+\tau} dW(t_1)e^{\mathcal{L}(t+\tau-t_1)}\mathcal{H}\left\{e^{\mathcal{L}(t_1-t)}\rho(t) + \int_t^{t_1} dW(t_2)e^{\mathcal{L}(t_1-t_2)}\mathcal{H}\left[e^{\mathcal{L}(t_2-t)}\rho(t) + \cdots\right]\right\}. \tag{B9}$$

This expression cannot be simplified into the usual Dyson sum because $\mathcal{H}$ is a nonlinear superoperator. Explicitly expanding the first superoperator $\mathcal{H}$, and using the abbreviation

$$\sigma(t_2) = e^{-\mathcal{L}(t_2-t)}\mathcal{H}\left\{e^{\mathcal{L}(t_2-t)}\rho(t) + \int_t^{t_2} dW(t_3)e^{\mathcal{L}(t_2-t_3)}\mathcal{H}\left[e^{\mathcal{L}(t_3-t)}\rho(t) + \cdots\right]\right\}, \tag{B10}$$

gives the following:

$$\begin{aligned}\rho_c(t+\tau) = e^{\mathcal{L}\tau}\rho(t) + \sqrt{\gamma\eta}\int_t^{t+\tau} dW(t_1)e^{\mathcal{L}(t+\tau-t_1)} \\ \times\Bigg(ae^{\mathcal{L}(t_1-t)}\left[\rho(t) + \int_t^{t_1} dW(t_2)\sigma(t_2)\right] + e^{\mathcal{L}(t_1-t)}\left[\rho(t) + \int_t^{t_1} dW(t_2)\sigma(t_2)\right]a^\dagger \\ - \mathrm{Tr}\left\{(a+a^\dagger)e^{\mathcal{L}(t_1-t)}\left[\rho(t) + \int_t^{t_1} dW(t_{2;1})\sigma(t_{2;1})\right]\right\} \\ \times e^{\mathcal{L}(t_1-t)}\left[\rho(t) + \int_t^{t_1} dW(t_{2;2})\sigma(t_{2;2})\right]\Bigg).\end{aligned} \tag{B11}$$

From this it is evident that the full expansion of (B9) contains products of infinitesimal Weiner increments of the form

$$dW(t_1)[dW(t_{2;1})\cdots dW(t_{2;m_2})][dW(t_{3;1})\cdots dW(t_{3;m_3})]\ldots, \tag{B12}$$

where $m_2, m_3, \ldots$ are unspecified natural numbers. Now, because of the time ordering in (B9) and the nature of the Ito calculus, the time arguments in products such as (B12) can be considered to satisfy the following strict inequalities:

$$t_1 > t_{i;j} \geq t \quad \text{for } i \geq 2. \tag{B13}$$

There are two particular points to note about this. Firstly, $dW(t_1)$ is independent of $dW(t_{i;j})$ for $i \geq 2$, and so will always nullify an ensemble average unless paired with some other stochastic term. Secondly, $t_1 > t$ unless $m_2 = m_3 = \cdots = 0$. Thus we have

$$\langle\xi(t)dW(t_1)[dW(t_{2;1})\cdots dW(t_{2;m_2})][dW(t_{3;1})\cdots dW(t_{3;m_3})]\cdots\rangle_E = 0 \tag{B14}$$

unless $t_1 = t$, which requires $m_2 = m_3 = \cdots = 0$. When this is satisfied, we get

$$\langle\xi(t)dW(t_1)\rangle_E = \delta(t_1 - t)dt_1. \tag{B15}$$

Now the expansion (B9) for $\rho_c(t+\tau)$ truncated at the first stochastic term is

$$\rho_c(t+\tau)^{(1)} = e^{\mathcal{L}\tau}\rho(t) + \int_t^{t+\tau} dW(t_1)e^{\mathcal{L}(t+\tau-t_1)}\mathcal{H}[e^{\mathcal{L}(t_1-t)}\rho(t)]. \tag{B16}$$

Thus we have

$$\begin{aligned}\langle\rho_c(t+\tau)\xi(t)\rangle_E &= \int_t^{t+\tau} dt_1\delta(t-t_1)e^{\mathcal{L}(t+\tau-t_1)}\mathcal{H}\,e^{\mathcal{L}(t_1-t)}\rho(t) \\ &= \sqrt{\gamma\eta}e^{\mathcal{L}\tau}[a\rho(t) + \rho(t)a^\dagger - \mathrm{Tr}[a\rho(t) + \rho(t)a^\dagger]\rho(t)],\end{aligned} \tag{B17}$$

where we have used the definition of $\mathcal{H}$ (B5). Substituting this into (B2) gives

$$F(t;\tau) = \sqrt{\gamma\eta}(\mathrm{Tr}\{X_1 e^{\mathcal{L}\tau}[a\rho(t) + \rho(t)a^\dagger]\} - \mathrm{Tr}\{X_1 e^{\mathcal{L}\tau}[\rho(t)]\}\mathrm{Tr}\{(a+a^\dagger)\rho(t)\})$$
$$= 2\sqrt{\gamma\eta}(\mathrm{Tr}\{: X_1 e^{\mathcal{L}\tau}[X_1\rho(t)] :\} - \mathrm{Tr}\{X_1 e^{\mathcal{L}\tau}[\rho(t)]\}\mathrm{Tr}\{X_1\rho(t)\}), \quad \text{(B18)}$$

where :: denotes normal ordering of annihilation and creation operators.

APPENDIX C: STOCHASTIC EVOLUTION EQUATION FOR THE P FUNCTION

In this appendix we derive the stochastic evolution equation for the P function under homodyne measurement and obtain some elementary results. From Eq. (4.24) we have the following expression for the infinitesimally evolved density operator:

$$\rho_c(t+dt) = \rho_c + \frac{\gamma}{2}dt(2a\rho_c a^\dagger - a^\dagger a\rho_c - \rho_c a^\dagger a) + \sqrt{\gamma\eta}dW(t)(a\rho_c + \rho_c a^\dagger - \langle a+a^\dagger\rangle_c\rho_c). \quad \text{(C1)}$$

Recall that η is the efficiency of the homodyne measurement. Now, $\rho_c = \rho_c(t)$ can be formally represented by the Glauber-Sudarshan P function,

$$\rho_c = \int d^2\alpha\, P_c(\alpha,t)|\alpha\rangle\langle\alpha|. \quad \text{(C2)}$$

Substituting this into (C1) gives

$$\rho_c(t+dt) = \int d^2\alpha\, P_c(\alpha,t)[1+\gamma dt|\alpha|^2 + \sqrt{\gamma\eta}dW(t)(\alpha+\alpha^* - \langle a+a^\dagger\rangle_c)]\left(1-\frac{\gamma}{2}a^\dagger a dt\right)|\alpha\rangle\langle\alpha|\left(1-\frac{\gamma}{2}a^\dagger a dt\right). \quad \text{(C3)}$$

From the number-state expansion for the coherent states, it is easy to show that, to first order in the infinitesimal dt, $(1-\gamma a^\dagger a dt/2)|\alpha\rangle = (1-\gamma|\alpha|^2 dt/2)|\alpha e^{-\gamma dt/2}\rangle$. Substituting this into (C3) and changing the integration variable to $\alpha e^{-\gamma dt/2}$ yields the infinitesimally evolved P function

$$P_c(\alpha, t+dt) = e^{\gamma dt}P_c(\alpha e^{\gamma dt}, t)[1 + \sqrt{\gamma\eta}dW(t)(\alpha+\alpha^* - \langle a+a^\dagger\rangle_c)], \quad \text{(C4)}$$

as quoted in Sec. IV C.

From this, it is easy to determine the evolution of moments of X_1. For example,

$$\langle X_1\rangle_c(t+dt) = \int d^2\alpha\, P_c(\alpha, t+dt)\tfrac{1}{2}(\alpha+\alpha^*). \quad \text{(C5)}$$

Using expression (C4) and making the reverse variable change to that made above gives the infinitesimally evolved conditional mean of X_1 as

$$\langle X_1\rangle_c(t+dt) = e^{-\gamma dt/2}\langle X_1\rangle_c(t) + 2\sqrt{\gamma\eta}dW(t)\left[\int d^2\alpha\, P_c(\alpha,t)\tfrac{1}{4}(\alpha+\alpha^*)^2 - \tfrac{1}{4}\langle a+a^\dagger\rangle_c^2(t)\right]. \quad \text{(C6)}$$

The term in square brackets may be recognized as the variance in X_1 minus a constant $\frac{1}{4}$ which arises when the operator X_1^2 is put in normal order. Writing the normally ordered variance as $u_c(t)$ gives (C6) in the form quoted in Sec. IV C.

APPENDIX D: ALTERNATIVE APPROACHES TO QUANTUM TRAJECTORIES

Here we compare Carmichael's "quantum trajectories" [7,8] with other approaches to the stochastic state vector evolution. The first alternative is the theory of Gardiner, Parkins, and Zoller [18], with examples given in Refs. [16, 17]. They consider the general master equation of the form

$$\dot\rho = \frac{1}{i\hbar}[H,\rho] + \sum_\gamma (C_\gamma\rho C_\gamma^\dagger - \tfrac{1}{2}C_\gamma^\dagger C_\gamma\rho - \tfrac{1}{2}\rho C_\gamma^\dagger C_\gamma), \quad \text{(D1)}$$

where the various system operators C_γ arise from irreversible coupling to various reservoirs. The solution to this may be written as

$$\rho(t) = \sum_{n=0}^{\infty}\int_0^t dt_n \int_0^{t_n} dt_{n-1}\cdots\int_0^{t_2} dt_1\, \mathcal{S}(t-t_n)\mathcal{J}\mathcal{S}_1(t_n-t_{n-1})\cdots\mathcal{J}\mathcal{S}(t_1)\rho(0), \quad \text{(D2)}$$

where $\mathcal{S}(t)\rho = N(t)\rho N(t)^\dagger$, $N(t) = \exp[(\frac{1}{i\hbar}H - \frac{1}{2}\sum_\gamma C_\gamma^\dagger C_\gamma)t]$, and where $\mathcal{J} = \sum_\gamma \mathcal{J}_\gamma$, $\mathcal{J}_\gamma\rho = C_\gamma\rho C_\gamma^\dagger$. This expansion could also have been written, perhaps more intuitively, as a series of nested expansions in each $\mathcal{J}_\gamma$, as was done in Sec. V on balanced homodyne measurements. In any case, the method of simulation is the same as outlined in that section. A random time to the next jump is computed from the waiting time distribution, the system ket is evolved via $N(t)$ up to that time, and then a jump process C_γ is applied, chosen randomly using the weights $\langle C_\gamma^\dagger C_\gamma\rangle$.

Although equivalent in derivation, the interpretation of such a simulated system ket is different from that in Carmichael's theory in its strict form (see the end of Sec. II). This is because the operators C_γ do not necessarily represent output fields incident on a photodetector. Thus the simulated ket is not conditioned on known events and rather is a purely formal device for reproducing the system evolution. In the case of a cavity coupled to one reservoir in the vacuum state, the history of the system is the same as for standard photodetection (Sec. II), as both theories then coincide with that of Srinivas and Davies [1]. However, it is only with the interpretation of the simulation as representing an actual (conditioned) quantum trajectory that it makes sense to add a local-oscillator amplitude to the collapse operator (Sec. IV), or to consider ensemble averages such as $\langle\langle X_1\rangle_c^2\rangle_E$.

The method of Teich and Mahler [19] for treating irreversible evolution using ket vectors is quite different from that above. It involves splitting the master equation dynamics into two parts: coherent, which smoothly changes the instantaneous diagonal basis of the density operator, and incoherent, which causes the system to jump between these eigenstates according to rate equations. This scheme is intuitively appealing because an eigenvalue of the density matrix can be regarded as the probabilities of the system actually being in the corresponding eigenstate. For stationary processes, the eigenstates are fixed in time and only jump processes occur.

In contrast with Gardiner, Parkins, and Zoller [18], Teich and Mahler [19] do make the claim that a stochastic simulation using their method represents the evolution of a single quantum system. Although this seems reasonable for the systems they consider (few-level atoms), it fails in optical systems. For example, the steady-state density operator for a single-mode laser is diagonal in the photon-number eignestates. By Teich and Mahler's theory, the mode would therefore always be in such a state, with completely indeterminate phase. However, the master equation for the laser is unchanged if its output is subject to homodyne detection, yet this clearly will extract phase information. Thus the ensemble of kets which recreates the density operator will not necessarily consist of its eigenstates, and the jump processes which may occur in a quantum trajectory are more general than those considered by either Teich and Mahler or Gardiner, Parkins, and Zoller.

[1] M.D. Srinivas and E.B. Davies, Opt. Acta **28**, 981 (1981).
[2] W. Pauli, *General Principles of Quantum Mechanics* (Springer-Verlag, Berlin, 1980).
[3] W.H. Richardson and Y. Yamamoto, Phys. Rev. A **44**, 7702 (1991).
[4] P. Storey, M.J. Collett, and D.F. Walls, Phys. Rev. Lett. **68**, 472 (1992).
[5] R.J. Glauber, Phys. Rev. **130**, 2529 (1963); **131**, 2766 (1963).
[6] E.C.G. Sudarshan, Phys. Rev. Lett. **10**, 277 (1963).
[7] H.J. Carmichael and L. Tian, in *Optical Society of America Annual Meeting Technical Digest 1990*, Optical Society of America Technical Digest Series Vol. 15 (Optical Society of America, Washington, DC, 1990).
[8] H.J. Carmichael (unpublished).
[9] C.W. Gardiner and M.J. Collett, Phys. Rev. A **31**, 3761 (1985).
[10] H.J. Carmichael, S. Singh, R. Vyas, and P.R. Rice, Phys. Rev. A **39**, 1200 (1989).
[11] P. Alsing, G.J. Milburn, and D.F. Walls, Phys. Rev. A **37**, 2970 (1988).
[12] I.K. Mortimer and H. Risken (unpublished).
[13] H.J. Carmichael, J. Opt. Soc. Am. B **4**, 1588 (1987).
[14] C.W. Gardiner, *Handbook of Stochastic Methods* (Springer-Verlag, Berlin, 1985).
[15] J.R. Klauder and E.C.G. Sudarshan, *Fundamentals of Quantum Optics* (Benjamin, New York, 1970).
[16] R. Dum, P. Zoller, and H. Ritsch, Phys. Rev. A **45**, 4879 (1992).
[17] R. Dum, A.S. Parkins, P. Zoller, and C.W. Gardiner, Phys. Rev. A **46**, 4382 (1992).
[18] C.W. Gardiner, A.S. Parkins, and P. Zoller, Phys. Rev. A **46**, 4363 (1992).
[19] W.G. Teich and G. Mahler, Phys. Rev. A **45**, 3300 (1992).
[20] L. Diosi, J. Phys. A **21**, 2885 (1988).
[21] N. Gisin, Helv. Phys. Acta **62**, 363 (1989).
[22] N. Gisin and I. Percival (unpublished).

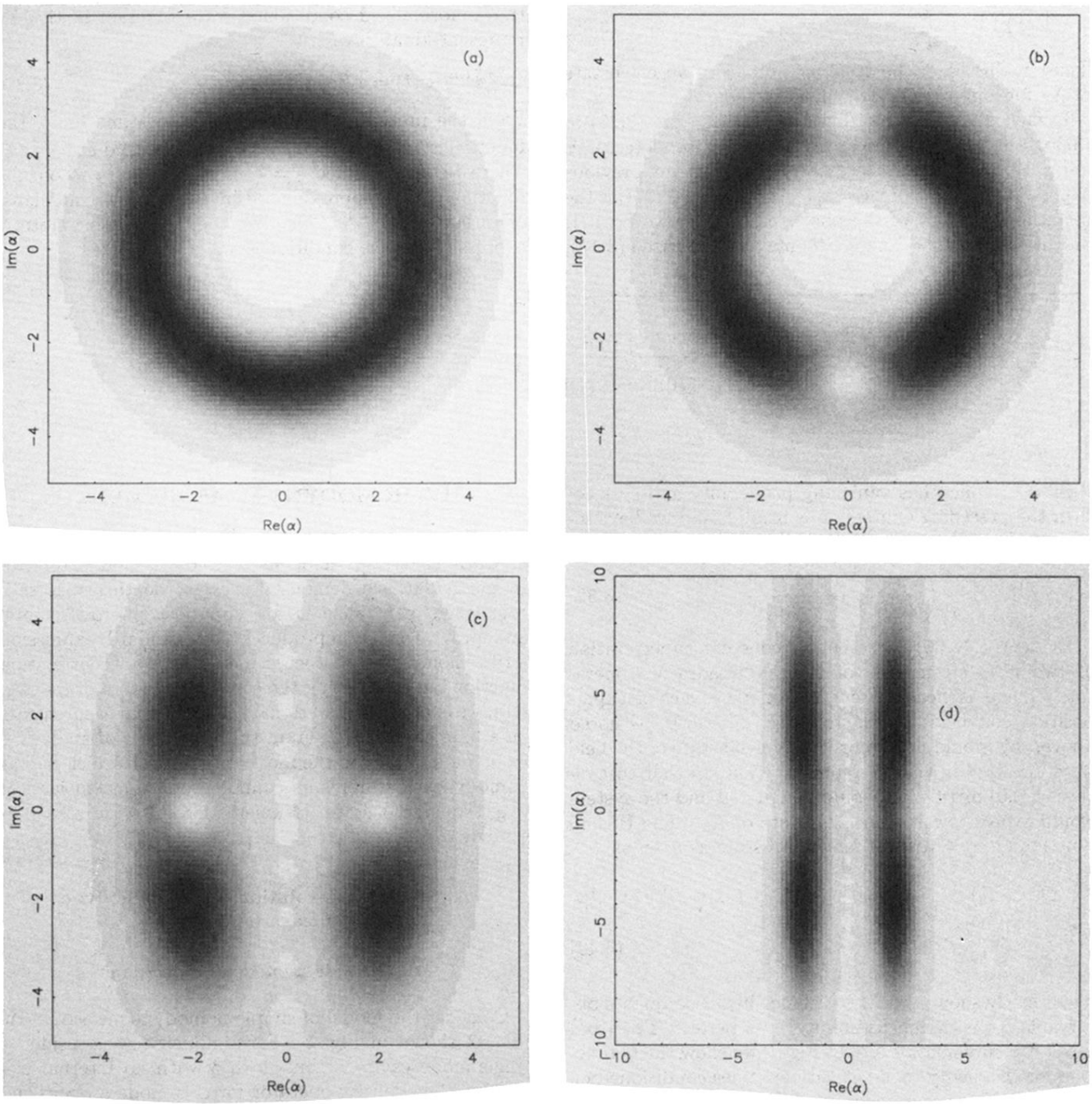

FIG. 2. Gray-scale plot of the Q function for the a mode conditioned on typical QND-measurement results. Initially (a) the system is in a Fock state $n = 8$. (b) shows the state at time $t = 0.25$ and photoncount $m = 1$; (c) at $t = 3.0$ and $m = 12$; and (d) at $t = 30$ and $m = 120$. Time is measured in inverse units of the measurement rate Γ.

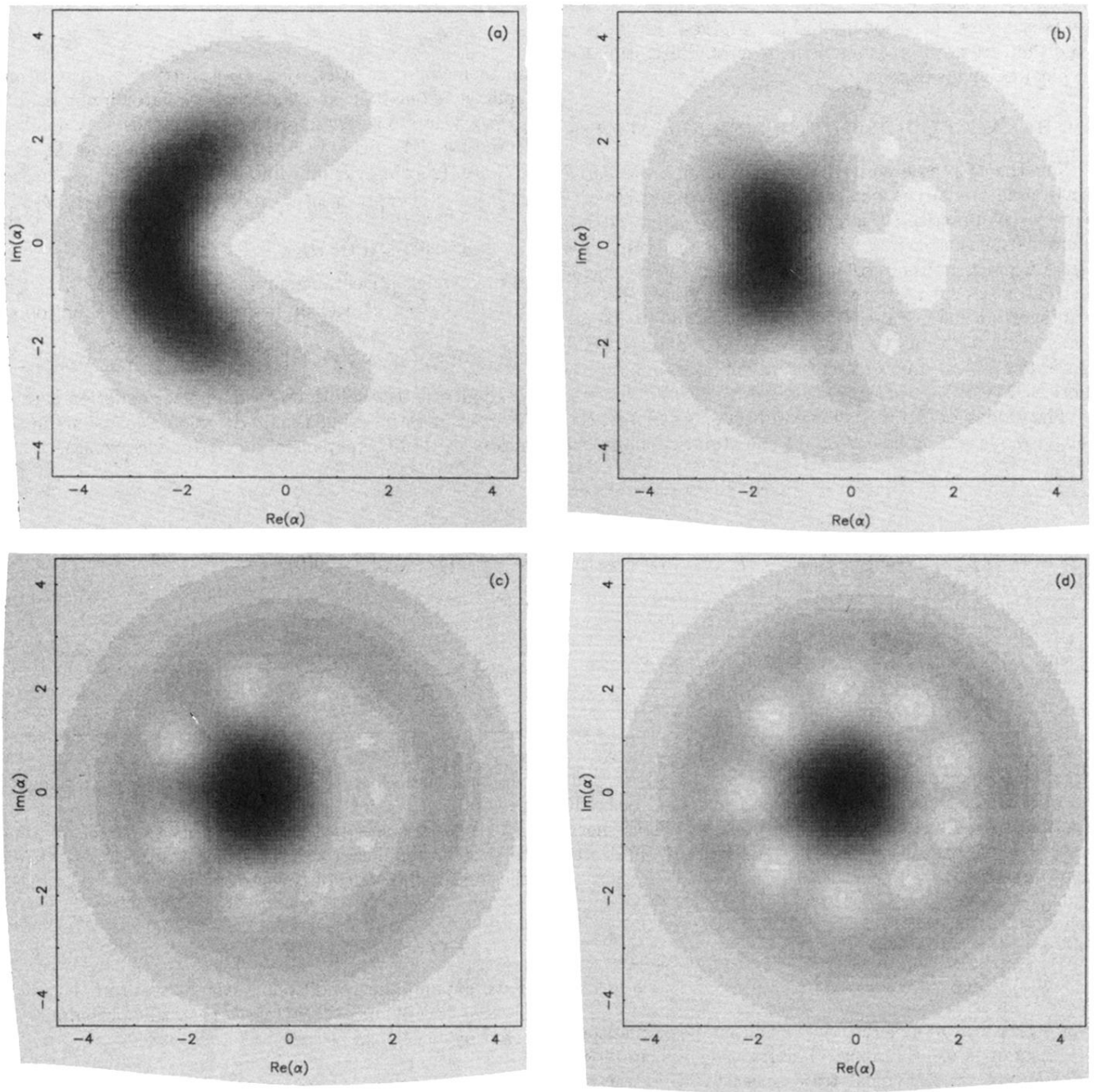

FIG. 9. Gray-scale plot of the Q functions for the cavity mode for a typical quantum trajectory under BHM. Here the initial condition [see Fig. 2(a)] is a Fock state $n = 8$ and the local oscillator is a coherent state $\beta = 100$. The times (measured in inverse units of the cavity linewidth γ) shown are (a) $t = 0.25$, (b) $t = 1.0$, (c) $t = 2.0$, (d) $t = 4.0$. The system at $t = 1.0$ is most squeezed, with an X_1 variance of 0.158.